

SCIENTIFIC DATA

OPEN

Data Descriptor: A database of biological and geomorphological sea-level markers from the Last Glacial Maximum to present

Received: 11 September 2017

Accepted: 13 March 2018

Published: 29 May 2018

F.D. Hibbert¹, F.H. Williams^{1,2}, S.J. Fallon¹ & E.J. Rohling^{1,2}

The last deglacial was an interval of rapid climate and sea-level change, including the collapse of large continental ice sheets. This database collates carefully assessed sea-level data from peer-reviewed sources for the interval 0 to 25 thousand years ago (ka), from the Last Glacial Maximum to the present interglacial. In addition to facilitating site-specific reconstructions of past sea levels, the database provides a suite of data beyond the range of modern/instrumental variability that may help hone future sea-level projections. The database is global in scope, internally consistent, and contains U-series and radiocarbon dated indicators from both biological and geomorphological archives. We focus on far-field data (i.e., away from the sites of the former continental ice sheets), but some key intermediate (i.e., from the Caribbean) data are also included. All primary fields (i.e., sample location, elevation, age and context) possess quantified uncertainties, which—in conjunction with available metadata—allows the reconstructed sea levels to be interpreted within both their uncertainties and geological context.

Design Type(s)	data integration objective • error correction objective
Measurement Type(s)	sea level
Technology Type(s)	data item extraction from journal article
Factor Type(s)	geographic location • proxy sensor • temporal_interval • elevation
Sample Characteristic(s)	Australia • New Zealand • Austral Islands • Gambier Islands • Society Islands • Tuamotu and Gambier Islands Subdivision • Lower Cook Islands • South America • Indian Ocean • Indian subcontinent • Southern Africa • Southeast Asia • Caribbean Region

¹Research School of Earth Sciences, The Australian National University, Canberra, ACT 2601, Australia. ²Ocean and Earth Science, University of Southampton, National Oceanography Centre, Southampton SO14 3ZH, UK. Correspondence and requests for materials should be addressed to F.D.H. (email: fiona.hibbert@anu.edu.au).

Background and Summary

Curated and complete archiving (i.e., with full observational and geochemical metadata) of indicators of former sea levels from multiple archives (e.g., corals, salt marshes, shorelines) is essential not only to address questions related to past changes in sea level, but also to couch current and future changes within a wider geological context. There is no single repository used by the community to archive information, and data are often drawn from disparate publications and repositories, with different data quality standards for each sub-discipline. Here we bring together published sea-level data from a wide range of sub-disciplines that encompass both biological and geomorphological archives.

Consistent treatment of each of the individual records in the database, and incorporation of fully expressed uncertainties, allows datasets to be easily compared. We focus on the transition from the last glacial to the current interglacial period, which is relevant to our understanding of future extreme sea-level change because it provides a suite of data beyond the range of modern/instrumental variability with which to robustly test simulations^{1–4}. Notably, the interval incorporates the last deglaciation, the most recent period of widespread destabilisation and collapse of major continental ice sheets. In model-based projections of future sea-level change⁵, the contribution of polar ice-sheet collapse is associated with large uncertainties, for example, regarding the rates and mechanisms of response to climate forcing. Past sea-level records provide some constraint on the natural bounds to the rates and magnitudes of polar ice-sheet decay^{6–8}. Our overarching goal therefore is to establish an open-source, community-led archive that will accelerate research on the rates and magnitude of past sea-level change through the interval of time for which the most detailed information exists.

Spatially, the database is global in scale, with a focus on far-field sites (Fig. 1). We concentrate on far-field sites, because other compilations are available for near-field sites, mainly based on salt marsh samples^{9–11}. We currently include microatoll data only where we are able to relate the elevation to a tidal datum, as we lack sufficient expertise to fully assess the physical and ecological relationship of this indicator to sea level. Temporally, the database concentrates on the interval 0 to 25 ka. At present, the database incorporates both U-series and radiocarbon dated samples. The database will be continually maintained and updated.

The compilation contains 194 studies (Table 1 (available online only)) from 40 locations (~2,600 data points) and includes all raw information and metadata, in contrast to other compilations where only a finalised age and relative sea level is given. This dataset complements and enhances the dataset of Hibbert *et al.*¹², adding different types of sea-level indicators (e.g., mangroves, bivalves and gastropods) and incorporating both radiocarbon and U-series dating methods. The present compilation contains ~2,600 sea-level markers for the past 25 ka, compared to 630 in Hibbert *et al.*¹².

Four broad types of information are required to reconstruct former relative sea levels^{13–15}: (1) location (including tectonic setting); (2) sample elevation and uncertainty; (3) sample age and uncertainty; (4) sample information and context, which includes how the sample relates to sea level at the time of formation. The inclusion of all available data (i.e., published, with some clarification from authors, where necessary) and associated uncertainties in these four categories, for each dataset in the compilation, places the sea-level indicators within a well-defined wider environmental context. This aids interpretation and ensures the continued utility and value of each contributing dataset. In addition, as all available ‘raw’ age data are included for both U-series and radiocarbon dated samples (e.g., activity ratios, spike calibration, decay constants, corrections applied), users are able to recalculate ages for the samples, if desired, which ensures continued utility of the data into the future.

No correction has been made for glacio-isostatic (GIA) processes. Instead, we present relative sea level records with extensive documentation, and refrain from making any interpretations. However, when the database is applied, GIA considerations and corrections will become necessary.

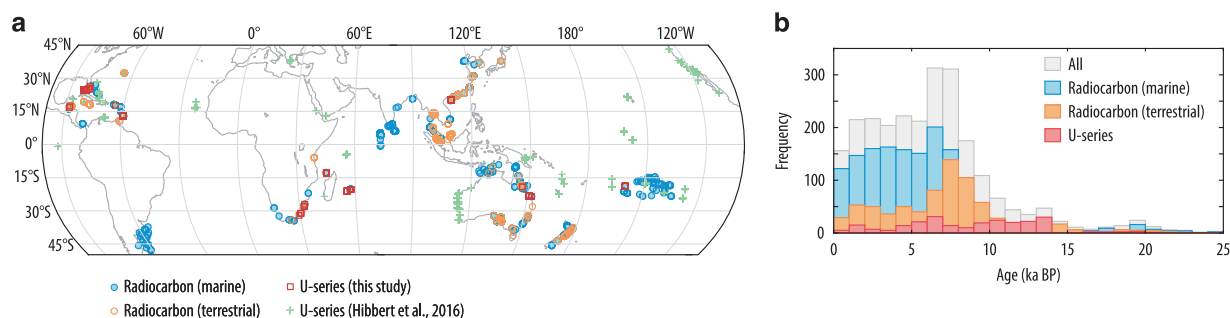


Figure 1. Location and age of fossil samples within the database. (a) Location of fossil samples: U-series dates (this study, red, open squares; Hibbert *et al.*¹², green crosses); marine radiocarbon (blue, filled circles) and terrestrial radiocarbon samples (orange, open circles). (b) Age frequency of fossil samples: all samples in the database (Data Citation 1, grey); U-series (red); and radiocarbon dated (marine, blue; terrestrial, orange).

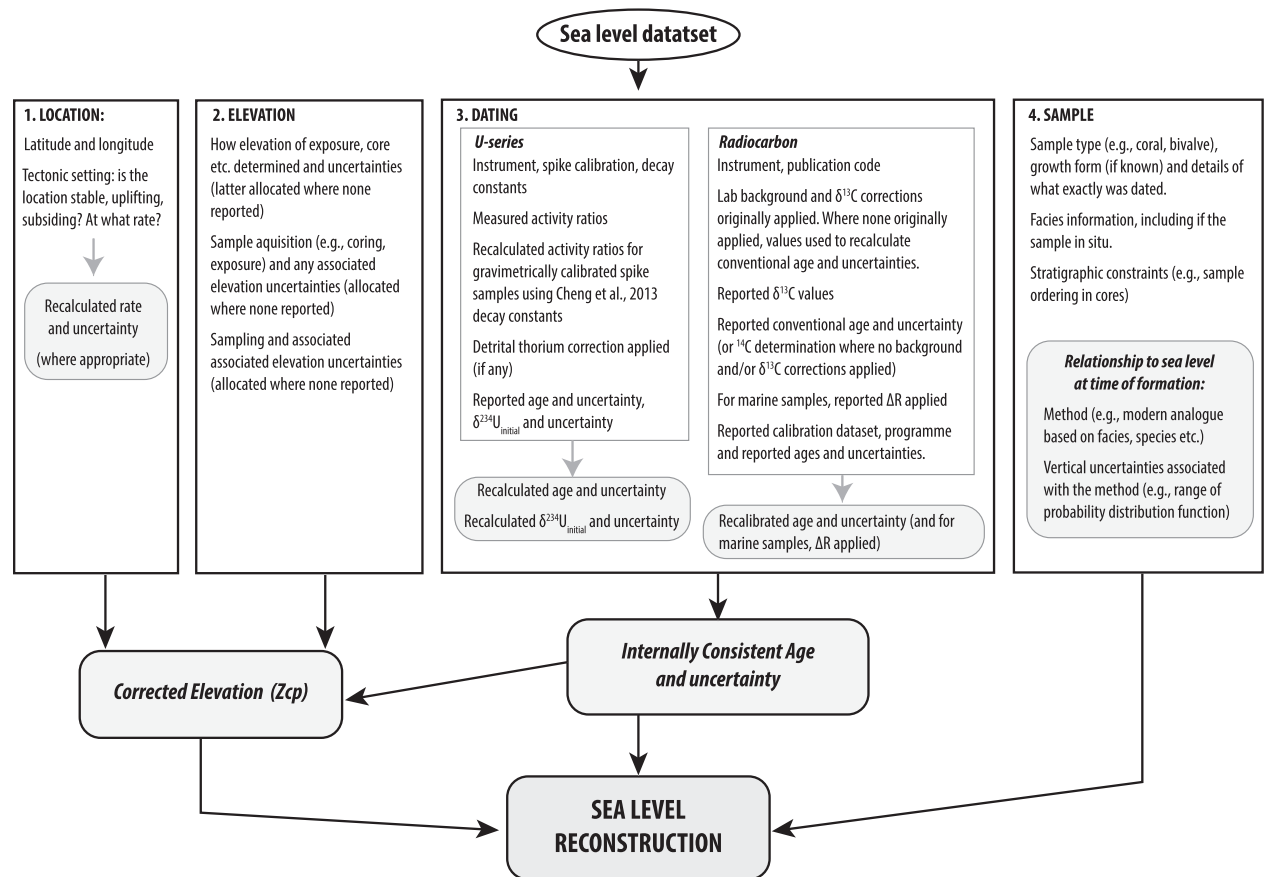


Figure 2. Simplified schema of the deglacial sea level database giving an overview of data acquisition and processing. The numbered boxes are the four essential components needed to reconstruct former sea levels: (1) location; (2) elevation; (3) age and; (4) sample information and other contextual information (including how the sample dated relates to sea level at the time of formation). Within each of these boxes we list the primary information recorded. Grey boxes indicate additional processing of data from original publications and new outputs (also included in the database, Data Citation 1).

Methods

All data have been obtained from peer-reviewed papers and books. Authors were contacted where information was missing or clarification was needed. Samples that still fail to reach a complete set of database fields have been excluded from our relative sea-level reconstructions. However, such samples are retained in the database because they may be important for other analyses. Figure 2 summarises the treatment of datasets within the database, and a brief outline of data acquisition and processing is given below.

Location

Each data point in the database has been assigned a unique identifier, along with the original sample or analysis identifier. Sample locations are as originally reported. Where this information was lacking or insufficiently detailed, the latitude and longitude were estimated.

Tectonic setting

The tectonic setting of a sample affects the reconstructed sea level through the interaction of uplift or subsidence with the measured elevation. Ideally, uplift/subsidence rates should be independently constrained. However, only Tahiti^{16,17} and Mururoa Atoll¹⁸ have such independent constraints. For most sites, the rates are often determined using the maximum elevation of the fossil coral terrace corresponding to the Last Interglacial, and an assumed age and relative sea-level position for the Last Interglacial. Occasionally, independent data (e.g., radiometrically dated lava flows) constrain the uplift/subsidence rate and we use these constraints where available (Mururoa Atoll¹⁹; Tahiti^{17,20,21}). Where no independent constraints are available, we have recalculated the uplift rates from the elevation of the maximum Last Interglacial terrace and an assumed Last Interglacial age and sea level (Table 2 (available online only), as per Hibbert *et al.*¹²).

Method	Max. quoted uncertainty (m, $\pm 2\sigma$)	Min. quoted uncertainty (m, $\pm 2\sigma$)	Allocated uncertainty (m, $\pm 2\sigma$)	derivation
1. Elevation determination:				
Auto-level	not reported	not reported	0.03	cf. levelling uncertainty (Törnqvist <i>et al.</i> ²² ; Hijma <i>et al.</i> ²⁹⁶)
clinometer and analog depth recording	not reported	not reported	half modern tidal range	n/a
digital depth gauge/ dive computer	not reported	not reported	0.5	Rovere <i>et al.</i> ²⁹⁷ ; Azzopardi and Sayer ²⁹⁸
interpolation between contours on drainage plans	variable	variable	dependent on contour spacing	n/a
interpolation from topographic maps; no contour spacing given	variable	variable	0.5	n/a
levelling	1.5	0.01	0.03	Törnqvist <i>et al.</i> ²² ; Hijma <i>et al.</i> ²⁹⁶
levelling (laser)	0.15	0.15	0.03	Törnqvist <i>et al.</i> ²² ; Hijma <i>et al.</i> ²⁹⁶
ship—echosounder/not reported	not reported	not reported	half modern tidal range	n/a
'spirit level and folding ruler'	not reported	not reported	0.5	n/a
survey, not reported	n/a	n/a	0.5	n/a
theodolite	not reported	not reported	0.03	cf. levelling uncertainty (Törnqvist <i>et al.</i> ²² ; Hijma <i>et al.</i> ²⁹⁶)
unknown or not reported	n/a	n/a	0.5	n/a
2. Coring method:				
Auger or hand auger	not reported	not reported	0.05	cf. hand coring (Hijma <i>et al.</i> ²⁹⁶ ; Woodroffe ²⁹⁹)
horizontal push core	not reported	not reported	0.15	cf. vibracoring and rotary drilling (Hijma <i>et al.</i> ²⁹⁶ ; Morton and White ³⁰⁰)
hydraulic drill or piston core	not reported	not reported	0.15	cf. vibracoring and rotary drilling (Hijma <i>et al.</i> ²⁹⁶ ; Morton and White ³⁰⁰)
piston corer, Livingstone, split spoon or unspecified	not reported	not reported	0.15	cf. vibracoring and rotary drilling (Hijma <i>et al.</i> ²⁹⁶ ; Morton and White ³⁰⁰)
Russian corer	not reported	not reported	0.01	Woodroffe ²⁹⁹
star picket driver	not reported	not reported	0.15	cf. vibracoring and rotary drilling (Hijma <i>et al.</i> ²⁹⁶ ; Morton and White ³⁰⁰)
single tube sampler	not reported	not reported	0.15	cf. vibracoring and rotary drilling (Hijma <i>et al.</i> ²⁹⁶ ; Morton and White ³⁰⁰)
percussion drilling	not reported	not reported	0.15	cf. vibracoring and rotary drilling (Hijma <i>et al.</i> ²⁹⁶ ; Morton and White ³⁰⁰)
rotary drill	not reported	not reported	0.15	cf. vibracoring and rotary drilling (Hijma <i>et al.</i> ²⁹⁶ ; Morton and White ³⁰⁰)
SCARID drilling system	Not reported	not reported	0.1	Dennis Hubbard (pers. comm)
barge mounted drilling rig	not reported	not reported	0.15	cf. vibracoring and rotary drilling (Hijma <i>et al.</i> ²⁹⁶ ; Morton and White ³⁰⁰)
virbracore	not reported	not reported	0.15	Hijma <i>et al.</i> ²⁹⁶ ; Morton and White ³⁰⁰
gravity corer	not reported	not reported	0.15	cf. vibracoring and rotary drilling (Hijma <i>et al.</i> ²⁹⁶ ; Morton and White ³⁰⁰)
'rigging'—unknown	not reported	not reported	0.15	cf. vibracoring and rotary drilling (Hijma <i>et al.</i> ²⁹⁶ ; Morton and White ¹⁹⁹⁷ ³⁰⁰)
drilling, unspecified	not reported	not reported	0.15	cf. vibracoring and rotary drilling (Hijma <i>et al.</i> ²⁹⁶ ; Morton and White ³⁰⁰)
not reported	0.5	0.03	0.15	cf. vibracoring and rotary drilling (Hijma <i>et al.</i> ²⁹⁶ ; Morton and White ³⁰⁰)
not reported, assumed hand coring	not reported	not reported	0.05	Hijma <i>et al.</i> ²⁹⁶ ; Woodroffe ²⁹⁹
not reported, assumed vibracoring	not reported	not reported	0.15	Brown ¹⁵⁴ ; Robbin ²⁵⁹
3. Sampling:				
author specified	0.001	2	n/a	n/a
cores	0.001	2	0.01	Shennan ¹⁴
exposure/outcrop	0.01	0.01	0.01	n/a
unknown/not reported setting	0.25	0.25	0.01	n/a

Table 3. Allocated elevation-, sample extraction- and sampling uncertainties (where these are missing from the original publication).

Sample elevation and uncertainty

The elevation uncertainty of a sample falls into two broad categories: (i) the measurement uncertainty related to the method used for establishing the elevation of the outcrop or core and (ii) sampling uncertainties associated with both the method of sample acquisition (e.g., core stretching or shortening errors), which is dependent upon the method, and uncertainties that arise from sampling a core or section. Where information is missing in the original publication, we allocate a method-appropriate uncertainty. For example, where there is no mention of how the elevation was obtained or where only the method is given (e.g., levelling), we allocate a ± 0.5 m and ± 0.03 m (cf. ref. 22) uncertainty (2σ),

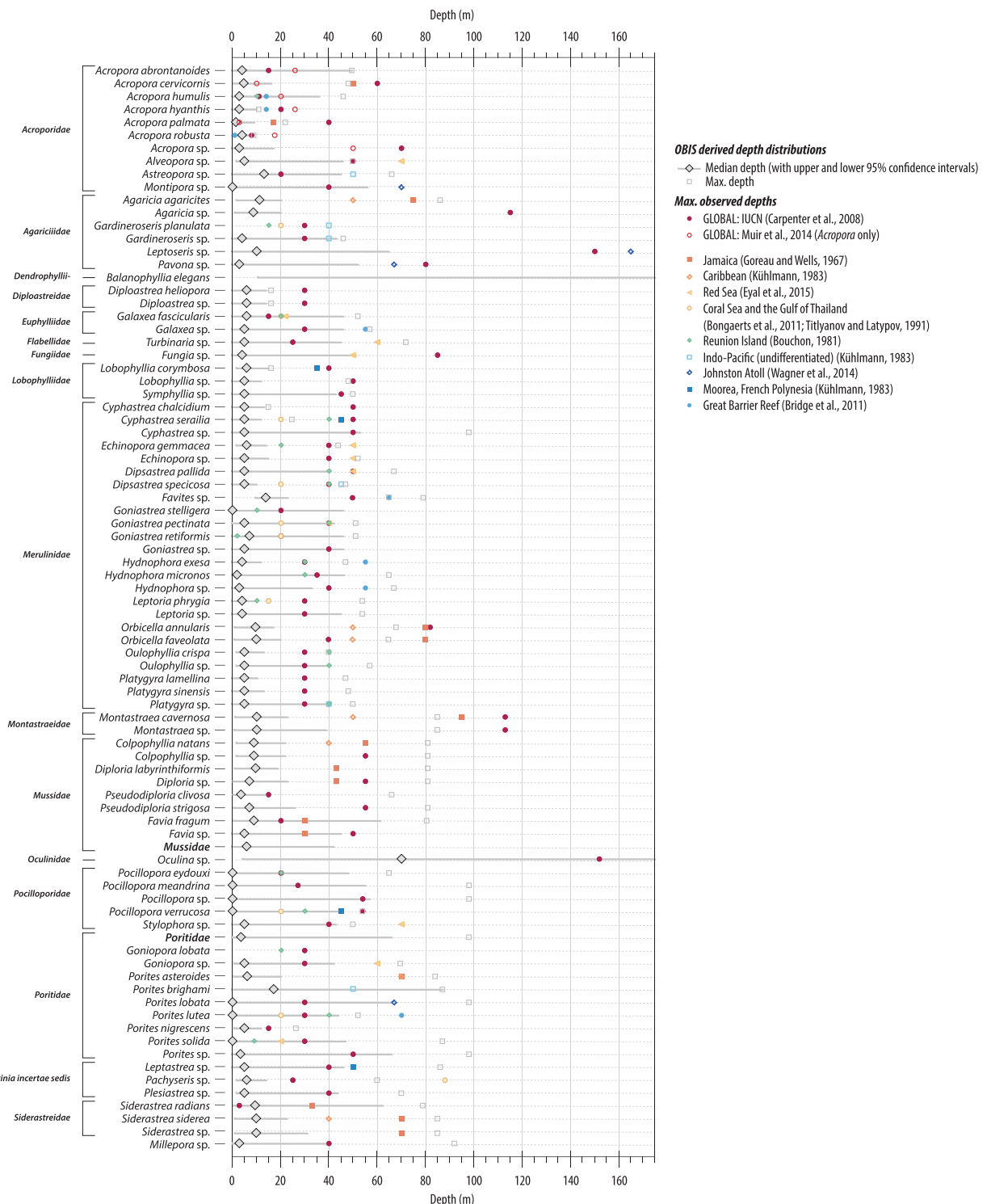


Figure 3. Coral depth distributions. Median (grey, filled diamond) and 95% confidence intervals (grey horizontal bars) for the ecologically derived depth distributions. The ICUN⁸⁹ global estimates of maximum depth (dark red, filled circles) and those derived for *Acropora* sp.⁹⁰ (red, open circles) are given for comparison. Also plotted are the maximum depths for certain recorded at various locations: Jamaica⁷⁵ (orange, filled squares); the Caribbean⁹² (orange, open diamonds); The Red Sea⁹⁷ (yellow, filled triangles); the Coral Sea⁹⁴ and Gulf of Thailand⁹³ (yellow, filled circles); Reunion Island⁹¹ (green, filled diamonds); the Indo-Pacific (blue, open squares); Johnston Atoll⁹² (dark blue, open diamonds); Moorea, French Polynesia⁹² (dark blue, filled squares) and; the Great Barrier Reef⁹⁵ (blue, filled circles).

respectively. Table 3 details the allocated uncertainties used in the database. The elevation uncertainty therefore is the root mean square of: (i) uncertainty associated with the method of establishing the elevation (e.g., levelling); (ii) uncertainties accounting for any distortion in obtaining the record (i.e., those resulting from coring methods) and; (iii) sampling uncertainties.

In order to compare elevations, a common datum is required. Within the database, we note the datum to which all measurements relate and, where possible, we reference all elevations to mean sea level (MSL) using appropriate tidal parameters (e.g., when converting elevations referenced to mean low water springs (MLWS) to MSL). We do not include any tidal errors; the modern tidal range often is not reported and variations in the past are poorly constrained.

Sample age and uncertainty

The database incorporates samples dated using U-series and radiocarbon methods. Detailed descriptions of the systematics of both these techniques are available elsewhere (e.g., for U-series dating^{23–25}; for radiocarbon dating^{26–28}). A brief summary of data type and processing is given in the following.

U-series analyses. We record the instrument, method of spike calibration, decay constants, activity ratios, and detrital thorium correction used in the original age determination (also included). For samples where the spike was calibrated gravimetrically, we recalculate the activity ratios using the most recent decay constants²⁹. For all samples, we then iteratively recalculate ages (equation 1) and $\delta^{234}\text{U}_{\text{initial}}$ (equation 2) assuming a closed system and using the most recent decay constants²⁹ (calculations were made using Isoplot v. 3.5 ref. 30). The reported uncertainties include the error associated with the decay constants.

$$1 - \left[\frac{{}^{230}\text{Th}}{{}^{238}\text{U}} \right]_{\text{act}} = e^{-\lambda_{230}T} - \left(\frac{\delta^{234}\text{U}_{(\text{meas})}}{1000} \right) \left(\frac{\lambda_{230}}{\lambda_{230} - \lambda_{234}} \right) \left(1 - e^{(\lambda_{234} - \lambda_{230})T} \right) \quad (1)$$

$$\delta^{234}\text{U}_{\text{initial}} = (\delta^{234}\text{U}_{\text{measured}}) e^{(\lambda_{234}T)} \quad (2)$$

where, $[{}^{230}\text{Th}/{}^{238}\text{U}]_{\text{act}}$ is the ${}^{230}\text{Th}/{}^{238}\text{U}$ activity ratio; λ_{238} , λ_{234} , λ_{230} are the decay constants of ${}^{238}\text{U}$, ${}^{234}\text{U}$ and ${}^{230}\text{Th}$ respectively^{29,31}; $\delta^{234}\text{U}_{(\text{meas})}$ is the measured value of the activity ratio of ${}^{234}\text{U}/{}^{238}\text{U}$ relative to secular equilibrium in per mille ($\delta^{234}\text{U} = ([{}^{234}\text{U}/{}^{238}\text{U}] - 1) \times 1000$); and T is the age of the sample in years.

We make no attempt to account for any open-system behaviour (i.e., the remobilisation of nuclides) within the U-series dated datasets because the identification and correction of open system behaviour continues to be complex and debated (e.g., ref. 24). In addition, we do not screen the recalculated ages for reliability; there are multiple approaches to assess age reliability and the inclusion of all metadata and the original reported ratios etc., allows users to determine appropriate age-reliability screening criteria (e.g., the bounds of acceptable $\delta^{234}\text{U}_{\text{initial}}$ values, % calcite etc.).

Ages are reported as ka BP in order to ensure that they are comparable to the radiocarbon ages, which are by convention reported as years before 1950 AD. We adjust the age for the time elapsed since analysis. Where no date of analysis is given, we have assumed this was the year of publication. We recognise that this may introduce additional age uncertainty but anticipate that this only a few years and typically less than a decade.

Radiocarbon analyses. We record the laboratory, instrument, publication code, any corrections applied by the laboratory (i.e., background and $\delta^{13}\text{C}$ corrections) and both the conventional and calibrated ages and associated uncertainties for each sample (including any regional marine reservoir age correction, ΔR , applied by the authors). We also report the $\delta^{13}\text{C}$ values for samples, and the calibration dataset and programme where provided. Where no background and/or $\delta^{13}\text{C}$ correction was applied by the laboratory, we apply a sample-specific normalisation (terrestrially derived organic material $\delta^{13}\text{C} = -25 \pm 2$ ‰; marine carbonates $\delta^{13}\text{C} = 0 \pm 2$ ‰). The conventional age can then be calculated using the appropriate (instrument dependent) ${}^{14}\text{C}/{}^{12}\text{C}$ or ${}^{14}\text{C}/{}^{13}\text{C}$ equations³². Age uncertainty is reported at the 1 σ level in accordance with standard radiocarbon reporting protocols^{33–35}.

We assume that sample materials obtained their carbon from only one reservoir (i.e., atmospheric or marine). Additionally, we assume that estuarine bivalve and mollusc samples are fully marine because additional information, such as $\delta^{18}\text{O}$ and $\delta^{13}\text{C}$ analyses, that would help establish the environment in which the sample was living is often not available. We recognise that there may be considerable variation in the regional marine reservoir correction (ΔR) for estuarine bivalve and mollusc samples due to the varying mixing of marine and freshwater^{36–39} which potentially results in an older apparent age for specimens living in estuarine environments.

A radiocarbon measurement requires an additional step of calibration to obtain an age estimate due to the non-linear nature of the ${}^{14}\text{C}$ timescale⁴⁰. Both the calibration procedure itself (given the complexity of the calibration dataset) and the choice of software and parameters (such as the use of Bayesian statistics to construct age-depth models)^{41,42} influence the final calibrated age of a sample.

The calibration curve may affect the statistical inference of time because the relationship between the radiocarbon age and the calendar age changes through time, due to variations in the radiocarbon concentration (e.g., refs 43,44). In addition, the shape of the calibration curve (non-monotonic with

inversions) means that calibration is non-commutative and directional⁴⁵, with distortions due to the structure of the curve itself⁴³, the potential for the production of artificial peaks⁴⁶, and the amplification of the output probability density function by steep sections of the calibration curve^{45,47}. This can result in the summed probability density function of a calibrated date exceeding the ‘true’ time interval of the event⁴⁸.

Different calibration algorithms may affect the final calibrated age probability distribution, particularly when comparing results from software packages that do, or do not apply Bayesian statistics, i.e., where the age-depth model uses different depositional models to mimic sediment deposition processes. For example, OxCal⁴⁹, BChron⁵⁰, and Bacon⁵¹ utilise Bayesian statistics to incorporate stratigraphic and other chronological information to formulate prior distributions for the calibrated dates, and to provide ‘best-estimate’ age-depth models with uncertainties. In the database, we have chosen not to implement such age-depth modelling routines for datasets with stratigraphic ordering when recalibrating the radiocarbon dates, for several reasons: (1) to ensure consistency within the database; (2) because not all samples in the database have simple stratigraphic relationships, for example, coral reefs are complex 3-dimensional structures that do not necessarily accumulate monotonically like sediment cores, and; (3) to refrain from imposing any structure on future analysis. Overviews and comparisons of the main age-depth modelling routines are available^{41,42}, should users wish to apply these on appropriate, individual subsets of the database. Samples with stratigraphic ordering are clearly identified in the database with a numeric identifier for each group, and ordering given by subdivision of that number, smallest/topmost to largest/lower-most sample.

The conventional radiocarbon age and uncertainty for each sample were recalibrated using OxCal version 4.3. (ref. 52) and the latest calibration datasets: IntCal13 (ref. 53) for northern hemisphere terrestrial samples; SHCal13 (ref. 54) for southern hemisphere terrestrial samples; and Marine13⁵³ for all marine samples. For marine samples, we apply a local marine reservoir correction (ΔR ⁵⁵) to account for regional variations in the offset between the marine and terrestrial carbon reservoirs (the marine reservoir effect). The marine reservoir effect (i.e., the offset in the radiocarbon age of marine materials compared to materials deriving their ¹⁴C from the atmospheric at the same time) is spatially and temporally variable. The spatial variation from a calculated global average is accounted for by using a regional offset (ΔR). A consistent value of ΔR was applied for each coherent geographical region (i.e., for all sites influenced by the same surface oceanographic circulation) and estimated from the online database⁵⁶, double checked with previous ΔR determinations (Table 4 (available online only)). The online database⁵⁶ of values (and calculations of ΔR ⁵⁷) is used to ensure both the correct and consistent calculation of ΔR . Note that the method used to calculate ΔR in the online database incorporates the full probability distribution unlike ‘classical’ intercept methods, so that the resulting ΔR uncertainties are more accurate (full discussion of the methodology⁵⁷). Where more than one ΔR value is used, we calculated an error weighted mean and uncertainty. We apply the pre-industrial calculated ΔR , but recognise that ΔR is also temporally variable^{58–60}. Applying a pre-industrial ΔR does not account for any variations through time as a result of changing climatic and surface-ocean conditions, or variations in the production of ¹⁴C in the atmosphere with variations in the Earth’s magnetic field e.g., ref. 61. In general, there are few locations in the database and a limited number of studies where the temporal variability in ΔR has been investigated. As this variability is largely unconstrained at present, we do not attempt to account for this uncertainty in the database but the effect would be most pronounced for sites with data spanning the transition from the glacial to interglacial, when reorganisations of ocean circulation and of carbon stores within the ocean may have led to potentially large variations in ΔR . It should be noted that any such age uncertainty may additionally affect the resulting P_{RSL} reconstruction of some sites through interaction with uplift or subsidence rates.

The output of a calibrated radiocarbon date is a probability density function. The calculated posterior probability distributions are often multimodal and difficult to summarise, except via graphical representations⁴¹. Reporting of the 68 and 95% confidence interval has become common, although not universal, in part due to the ease of plotting a point estimate. Point estimates (such as the mean, mode, median etc.) do not fully account for the variation in the output of calibration (i.e., the resulting multimodal distributions), and none of these point-based estimates can be considered a good estimate of the full complexity of the calibrated date^{44,62}. It is difficult within a database to accurately record the outcome of calibration. However, because all information required for calibration of a date is included in the database (*inter alia*: conventional radiocarbon date and uncertainty; material dated; ΔR for marine samples; calibration curve, programme and version), users can recalibrate the data and obtain the same probability density function as captured by the 68 and 95% confidence intervals listed in the database. The complete documentation also allows recalibration of the dates following future refinements of the calibration datasets, etc.

In our recalculation (where appropriate) and recalibration of radiocarbon samples, we take care to ensure that we round the calibrated age (to nearest whole number) only at the end of the process. However, we are unable to guarantee that is the case of the reported values used in each of the processing steps.

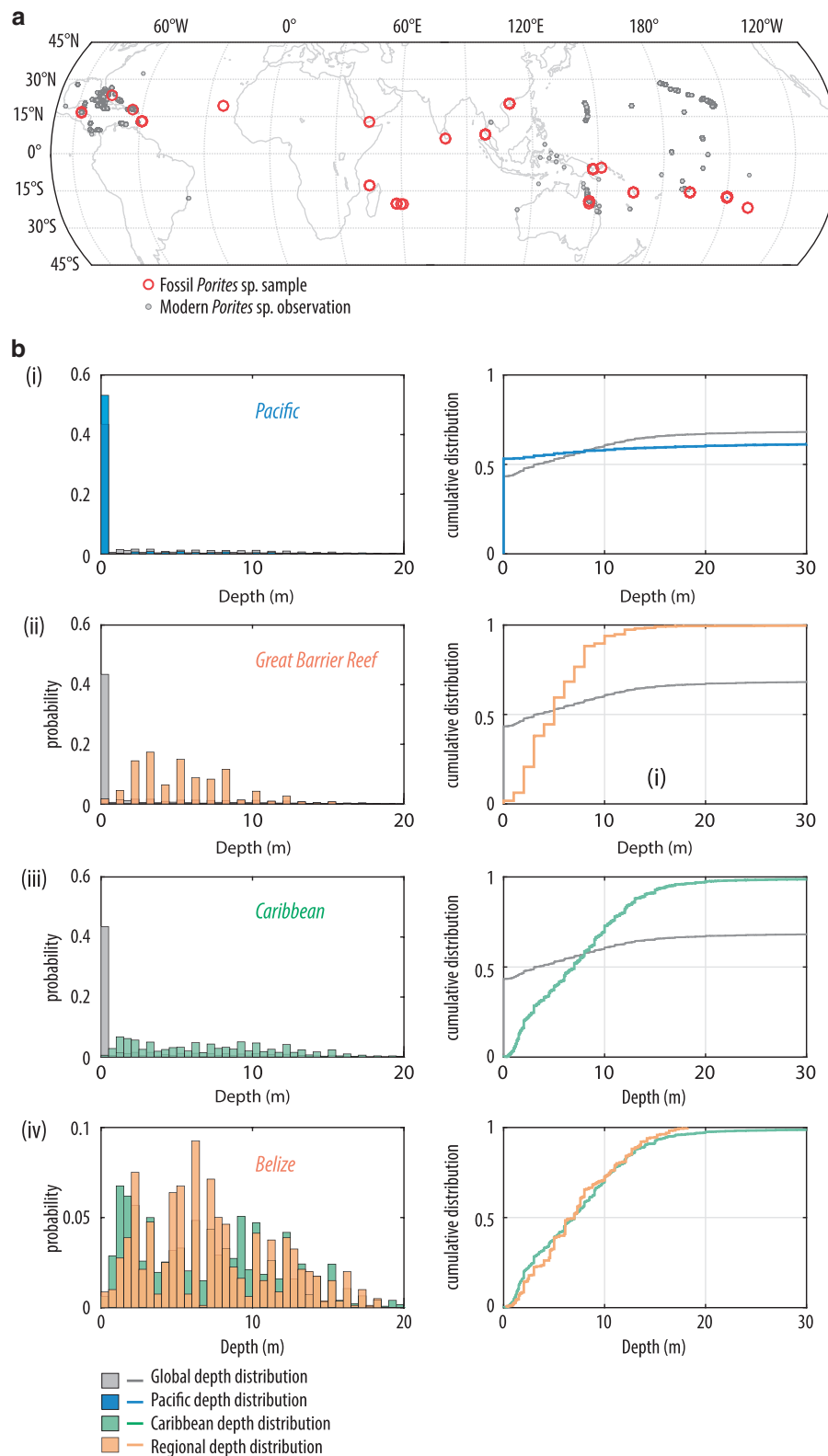


Figure 4. Modern observations of *Porites* sp. used to constrain depth distributions. (a) Map of fossil (red, open circles) and modern *Porites* sp. observations (plotted only those observations used to derived the depth distributions) (grey, filled circles). (b) Global (grey), basin and sub-basin (pink) depth distributions for *Porites* sp. represented as relative probability (normalised histograms, left panels) and cumulative frequency distributions (right panels): (i) ‘Global’ (grey) and Pacific (blue); (ii) ‘Global’ (grey) and Great Barrier Reef (orange); (iii) ‘Global’ (grey) and Caribbean (green); (iv) Caribbean (green) and Belize (orange).

Sample information and context

Detailed information on both the sample and its geological context is vital. We record available information from the publications including: what material was dated (and species, if given); the facies context and/or other outcrop and unit information; whether the authors determined the sample to be in growth position and/or *in situ*; and the growth form (e.g., branching or massive corals, if given).

In addition, to reconstruct past sea levels, we must establish the relationship between the sample and sea level at the time of its formation (i.e., the 'indicative meaning' which describes the range of elevations, with respect to a specified tidal datum, that a particular indicator forms^{13,14,63}). This is often achieved using a modern analogue, i.e., looking at the modern elevation range of a sea-level indicator in relation to present sea level (or some tidal datum). This approach is subject to key assumptions: (i) that the modern depth distribution is the most appropriate analogue; (ii) that the relationship is stable through time and; (iii) that the fossil record is a faithful approximation of the living diversity and distribution (i.e., minimal loss of detail due to taphonomic processes).

We use two different approaches for representing these relationships. The first uses a specific probability distribution for each taxon (e.g., the modern depth distribution of a coral species; following the methodology of Hibbert *et al.*¹²), and the second assumes a uniform probability distribution because the sea-level indicator forms somewhere within an altitudinal range but we have no further information as to the most likely depth or elevation (e.g., an oyster living somewhere within the intertidal to low-supratidal range at a given site).

Using a specific probability distribution of a species. For coral sea-level indicators, we are able to define a probability distribution for the depth-habitat (using the methodology detailed in Hibbert *et al.*¹² and summarised here). In this iteration of our analysis, we update the datasets used to define each taxon-specific depth distribution using the latest release from the Ocean Biogeographical Information System (www.iobis.org). The data in the OBIS dataset have been rigorously quality controlled. We use only observational and live-collected data with a vertical precision of ≤ 0.25 m. In some instances, there are insufficient observations (< 150) to constrain the depth distributions and so the depth precision criterion was relaxed: *Alveopora* sp. has a depth precision of ≤ 0.5 m ($n = 171$); *Favia fragum* and *Porites solidia* have a depth precision of ≤ 2 m ($n = 183$ and 149 respectively) and; *Acropora abrontanoides* has a depth precision of ≤ 5 m ($n = 132$). For some fossil species used to reconstruct past sea levels (*Goniopora lobata* and *Gardinerosis planulata*), little or no modern observational data were available and, in these instances, we use the modern genus depth distributions. We urge caution where fewer than 150 observations constrain the depth distributions.

For each taxon, we derive an estimate of the median water depth in which the modern species lives (Fig. 3). We have chosen the median rather than the mean because the depth distributions are not Gaussian or symmetrical and because the mean is more sensitive to outliers. The lower and upper bounds of the 95 and 68% confidence intervals were also determined using the 2.5, 97.5, 16 and 84 percentiles, respectively (Table 5 (available online only)); all depth observations used can be found in Data Citation 2 so that users may 'draw' directly from the distribution, if desired). We compile depth distributions at a 'global' scale (i.e., using all information available for the species) as well as geographical subsets: ocean basin, sub-basin and, where sufficient information is available, regional subsets (for example, Atlantic, Caribbean, Belize or Pacific, SW Pacific, Great Barrier Reef). These regional distributions are included as a first-order approximation of the modern variability (both geographically and with depth) of coral taxon distribution^{64,65}. Our ecological depth distributions are especially useful for sites lacking site-specific assemblage work that would constrain the modern relationship between coral depth and sea level.

In general, there are very few observations in the Indian Ocean and so it was not possible to further constrain the depth distributions for this region.

In the Pacific, there are significant numbers of observations but once sub-divided into sub-basin and regional locations, only the Great Barrier Reef (GBR) has sufficient, systematic observations (i.e., regular recording of data to depths of ~ 10 m and greater) to allow determination of robust regional depth distributions. For the most of the Pacific region, despite large numbers of observations, there appears to be a shallow-water bias, with observations concentrated within the upper couple of meters (for example using *Porites* sp., Fig. 4). Additionally, there are too few observations to allow determination of regional depth distributions with any confidence, particularly for the east and southeast of the basin. The depth distributions determined for the GBR region are based on numerous observations and span a greater depth range than other Pacific observations. However, collating observations from such a large geographical area likely masks the modern complexity of coral distribution within the reef system e.g., refs 66–68. Nonetheless it represents a first step in refining sea-level reconstructions, by incorporating a first-order approximation of the geographic variation in coral diversity and distribution. It should be noted that at present there are relatively few fossil corals in the database from the Great Barrier Reef (GBR) itself ($n = 27$ but, of these, 15 have been determined only to the genus level). The similarity between reef ecology, distributions and growth forms between Vanuatu and the GBR⁶⁹ also allows us to use the GBR depth distributions to refine sea-level reconstructions for Vanuatu. This is especially useful given that most ($\sim 70\%$) fossil corals from Vanuatu do not have original water depth determinations from modern biozonation of corals, coralline algae etc.

In the Atlantic, there is a substantial number of observations, including for the Caribbean sub-basin and for many regional sites. This allows definition of several taxon-specific, regional depth distributions. Most of these regional depth distributions are constrained by at least 100 observations, with most regions having > 300 observations (see summary statistics in Table 6 (available online only)). For many regions within the Caribbean sub-basin, there are distinct differences in species depth preference (e.g., *Acropora palmata*, Fig. 5), with notable offsets to deeper or shallower habitats evident relative to the ‘global’ depth distributions. This likely represents spatial variations in the depth habitat of the species (given the site-specific factors governing coral distributions and diversity; see review of Hibbert *et al.*¹²) but may also be an artefact of sampling bias (i.e., shallow-water bias in sampling). For some Caribbean fossil samples (e.g., those from St Croix in the US Virgin Islands, Belize, and Panama), modern constraints on the relationship between (tectonically corrected) coral elevation and sea level at the time of formation (i.e., a palaeo-water depth relationship) are lacking. As such, the regional depth distributions generated here allow us to both reconstruct sea level, and to incorporate the modern complexity in the geographic variation in taxon depth preference. Without this information on the relationship between the sample and sea level at the time of its formation, only a (tectonically) corrected elevation could be calculated, not sea level.

It should be noted that both the ‘global’ and regional depth distributions are a ‘maximum’ representation of the vertical uncertainties associated taxon-specific depth distributions. Additional biological (e.g., associated species with a narrower depth range) or geomorphological (e.g., designation as reef crest facies) information might be used to reduce the total vertical range associated with the reconstructed sea levels, if such additional data were provided. Unfortunately, most samples currently lack such information.

The use of modern analogues (including our OBIS-derived depth distributions) to define the palaeo-water depth relationship has three primary caveats. First, for some sites the present may not be the most appropriate analogue due to human influences^{70,71}. For example, the modern coral fauna of Barbados is not representative of the Pleistocene reefs due to reef destruction and loss of coral species, particularly the mass mortality of once dense populations of *Acropora palmata*^{72,73}. Fortunately, given the number of fossil corals from Barbados in the database, the similarity between the recurrent patterns in species dominance and diversity observed between the raised reef terraces of Barbados and the living reefs of Jamaica^{74,75}, first recognised by Mesolella⁷⁶, justifies the use of modern regional depth distributions of Jamaica as an analogue for Barbados. Second, the fossil record may not faithfully capture the living reef assemblage and structure due to the potential for non-preservation and selective removal/alteration of material by physical, chemical and/or biological processes (i.e., taphonomic processes^{77–81}). Third, a key assumption is the constancy and stability of the palaeo-water-depth relationship through time and, although difficult to determine, there is some evidence from the Caribbean that the large stands of branching *A. palmata* that dominated for the last 0.5 Ma are the same as those documented in the Caribbean until the early 1980’s, when human-induced habitat changes forced major changes in community structure^{72,73}.

Using a facies formation range or biological indicative range. For the non-coral subset of samples, we use the depth range or facies formation depth range as determined by the original authors. Where this information is missing, we are unable to reconstruct past relative sea level. We assume a uniform distribution for the relationship, in that the indicator may occur equally anywhere within the given altitudinal range. Note, the original coral palaeo-water depth determinations would also have a uniform distribution, and could be treated in the same manner, if desired.

Limiting data. For some samples, we are only able to say confidently that sea level was above or below the (tectonically corrected) elevation of the sample at the time of its formation. For example, a fossilised tree provides an upper limit on sea level at the time of growth, in that sea level must have been lower than the elevation of the sample. This subset of data is included, although we are unable to confidently reconstruct relative past sea levels, as such data can be very useful for constraining models of glacio-isostatic processes.

(Tectonically) Corrected position (Z_{cp})

Where appropriate, the modern elevation of the sample is corrected for uplift or subsidence since the time of formation, ensuring consistency between sites. For each sample, we are able to calculate the (tectonically) corrected position¹² (Z_{cp}) (equation 3)

$$Z_{cp} = E_{sam} - \left(\frac{\Delta H}{\Delta t} * t_{sam} \right) \quad (3)$$

where, Z_{cp} is the tectonically corrected elevation in m, and negative values are below sea level, E_{sam} is the elevation of the sea-level indicator referenced to mean sea level (MSL), $\Delta H/\Delta t$ is the recalculated uplift or subsidence rate in m/ka, with increasing positive ages in kilo-years before present and; t_{sam} is the recalculated (and recalibrated in the case of radiocarbon analyses) age of the sample in ka, with increasing positive ages in kilo-years before present (ka BP).

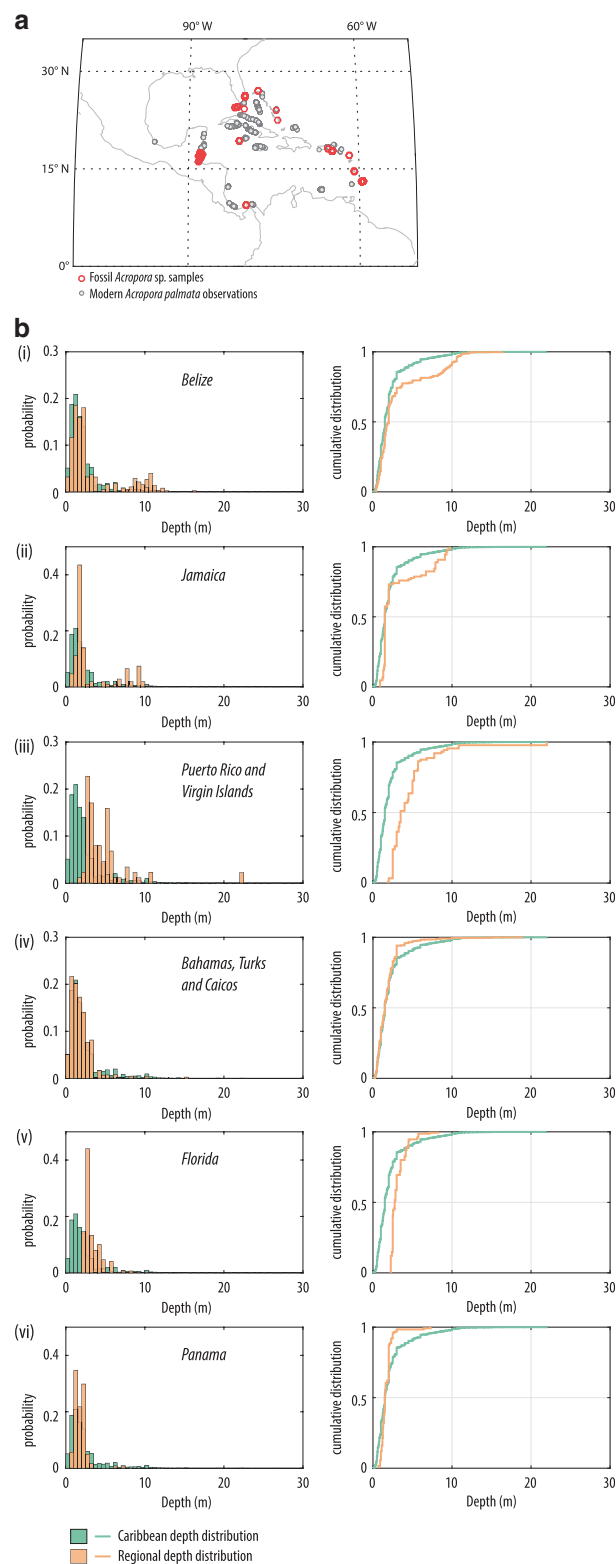


Figure 5. An example of regional depth distributions for *Acropora palmata* from the Caribbean sub-basin. (a) map of the fossil *Acropora* sp. samples (red open circles) and *A. palmata* observations used to constrain the depth distributions (grey, filled circles); (b) Caribbean depth distributions for *Acropora palmata* (green) and regional subsets (orange) represented as relative probability (normalised histograms, left panels) and cumulative frequency distributions (right panels).

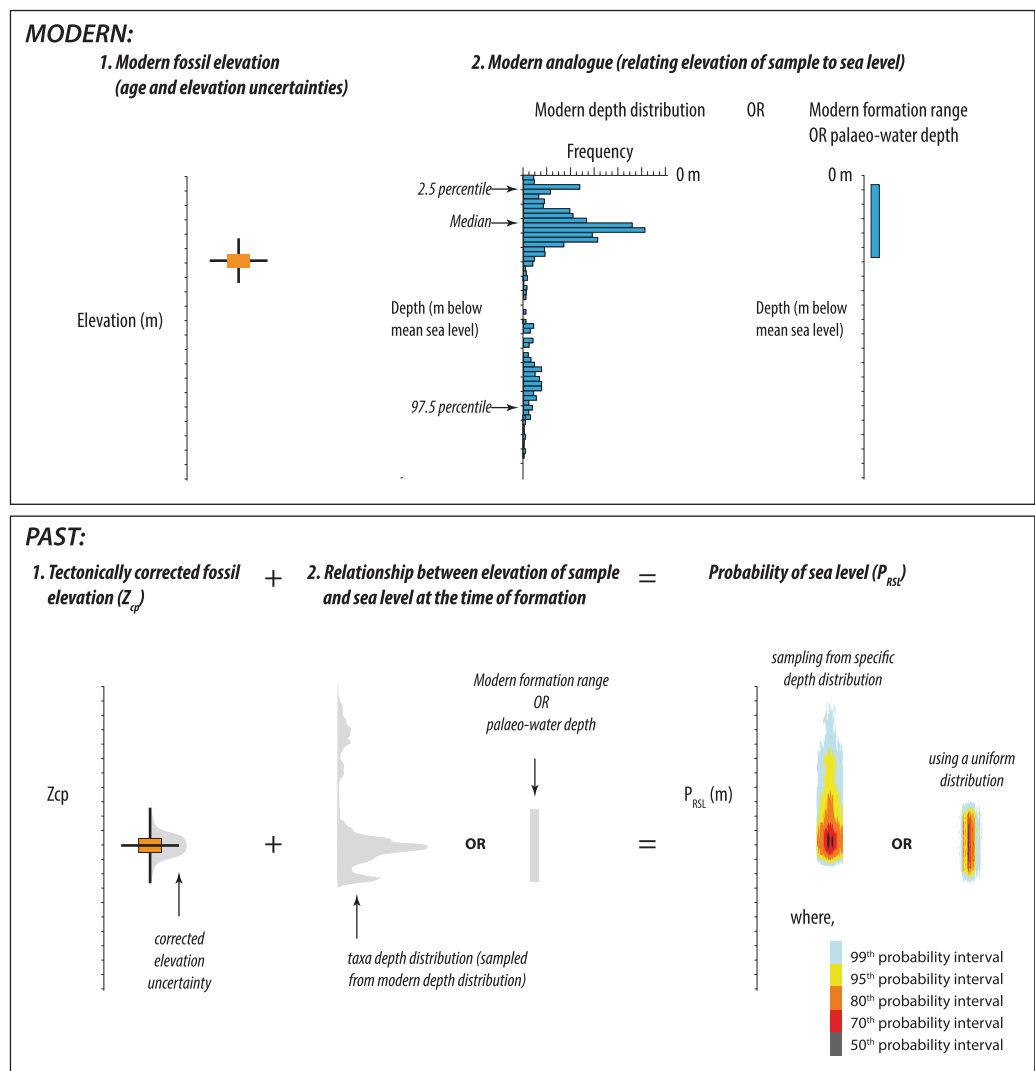


Figure 6. Schematic of relationship between, and uncertainty propagation for, the corrected coral position (Z_{cp}) and the probability of sea level (P_{RSL}).

Reconstructed Probability of Sea Level (P_{RSL})

We combine elevation uncertainties (including any uplift/subsidence correction) with the information relating the indicator to sea level at the time of formation (i.e., the modern altitudinal distribution for that indicator in relation to mean sea level) using the methodology of Hibbert *et al.*¹². A schematic of this procedure is given in Fig. 6. We use a Monte-Carlo approach of 350,000 simulations to derive a probability maximum (P_{RSL}) associated with each sea-level indicator position (Z_{cp}) and a confidence interval around that point. For each sea-level indicator, we obtain a set of randomly sampled values from the corrected position (Z_{cp}) uncertainty, and a set of randomly sampled values from the depth distribution (arising from either the empirically derived depth distributions for coral samples or a uniform distribution within a given formation range) and sum across the two errors. For each individual sea-level indicator, we then have multiple instances across a combined error distribution. From this set we can generate the probability distribution, and extract a probability maximum and the associated 1-, 2- and 3- sigma equivalent levels (68%, 95%, and 99% probability intervals) (the code used is provided, Data Citation 3). Note, these are typically asymmetrical for fossil coral samples when our modern, taxon-specific depth distributions are used to calculate P_{RSL} . Users of the database (Data Citation 1) are free to choose the relationship they deem most appropriate as we include the palaeo-water depth determined by the original authors, our OBIS-derived depth distributions (Data Citation 2), and the code (Data Citation 3) used to calculate P_{RSL} .

The result is a probability distribution of relative sea level (P_{RSL}) that incorporates both a eustatic, an isostatic and other (e.g., hydro-isostasy, compaction etc.) components. Note, we do not account for any glacio-isostatic processes as this is outside the scope of the present study. Additionally, we do not include any tidal corrections to our reconstructed sea levels to account for past variability in the magnitude and

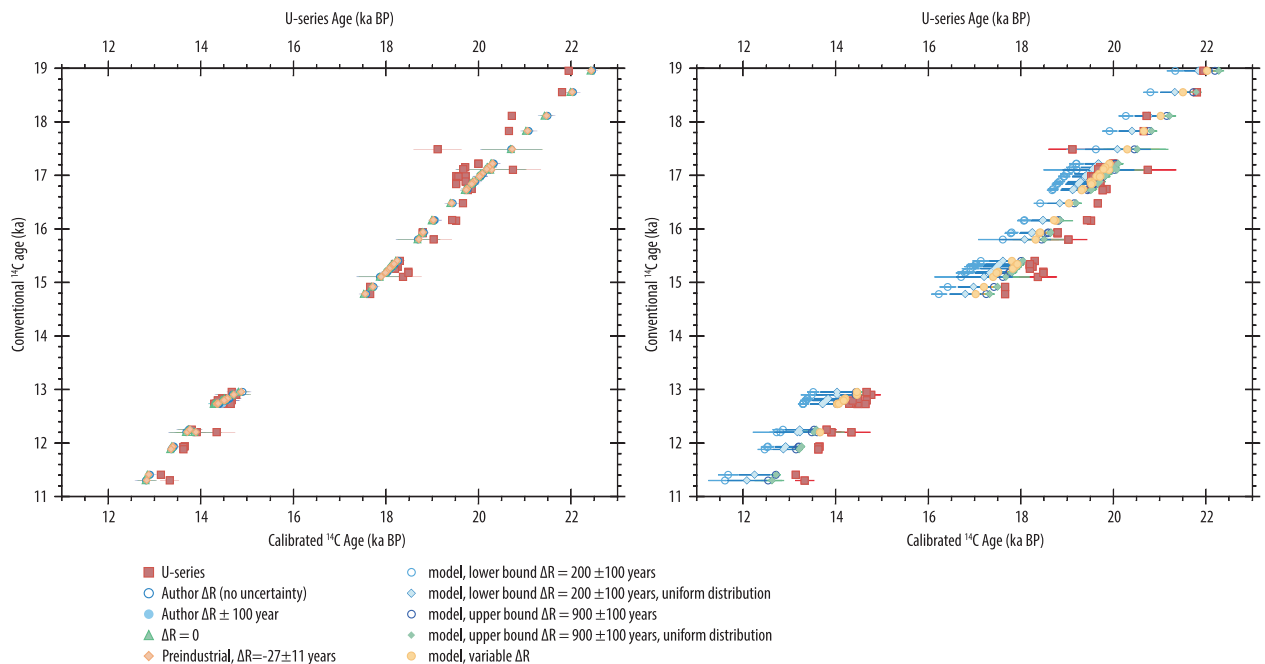


Figure 7. Investigation of the effect of variable ΔR on the calibrated age. This example uses corals from Barbados^{82,83} with both U-series and radiocarbon dates. U-series ages (red, filled squares) are recalculated assuming a closed system and the decay constants of Cheng *et al.*²⁹. Radiocarbon data are recalibrated using ΔR values: (left panel) of the original authors (dark blue, open circles); the original authors and a ± 100 year uncertainty (blue, filled circles); $\Delta R = 0$ (green, filled triangles) and preindustrial value of $\Delta R = -27 \pm 11$ years derived from Reimer and Reimer (ref. 56) (orange, filled diamonds). In the right panel, the U-series ages are compared to the recalibrated radiocarbon ages using ΔR values from the model of Butzin *et al.*⁸⁴: $\Delta R = 200 \pm 100$ years using a Gaussian (blue, open circles) and uniform (blue, filled diamonds) distribution; $\Delta R = 900 \pm 100$ years using a Gaussian (dark blue, open circles) and uniform (green, filled diamonds) distribution; a variable ΔR (yellow, filled circles).

spatial variation of past tidal regimes. In many publications, the modern tidal range is not reported and variations in the past are poorly constrained at present.

Data Records

The database (Data Citation 1) is designed to include all available data, for example we include all information relating to dating to enable users to recalculate the age, and associated metadata. ‘Data descriptors’ details all fields used in the database and can be found in Table 7 (available online only). The modern taxon-specific depth distributions (Data Citation 2) and the code (Data Citation 3) used to reconstruct past sea levels from fossil samples are also available from Figshare. A summary of the treatment of each the dataset in the database (Data Citation 1) can be found in ‘Supplementary Data’.

Technical Validation

In addition to ensuring consistency of data processing and any recalculations (age recalculation, recalibration etc.), we have attempted to validate various data-processing steps, where appropriate, and details for this are given below.

Age

Reported ages from the original publications are included in the database in addition to our recalculated ages (and recalibrated ages in the case of radiocarbon). This provides a first check of our age recalculations/recalibration. Note, that any uncertainty in the age determinations may propagate into our reconstructions of past relative sea-level through the interaction with uplift/subsidence.

U-series. All geochemical data are included in the database to enable users to recalculate the ages, if so desired. It should be noted that we do not screen the U-series ages for reliability. Users may select their own screening criteria (limits on acceptable $\delta^{234}\text{U}_{\text{initial}}$ values, calcite content etc.) from the fields included in the database (for examples, see ref. 12).

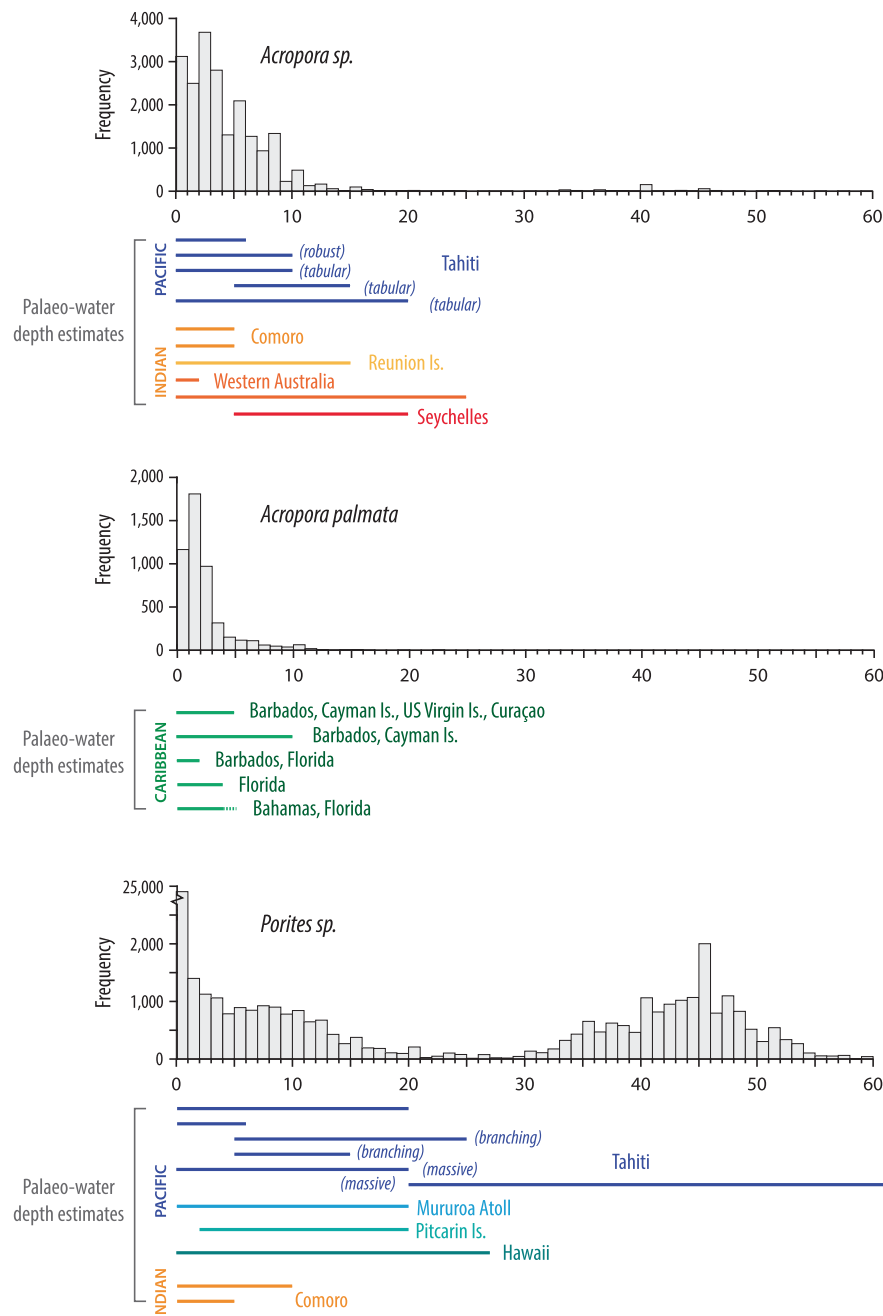


Figure 8. Coral depth distributions for three commonly dated species in the fossil database. The data uses observational and living data with a vertical depth precision of ≤ 0.25 m only. Coloured bars below each histogram are the palaeo-water depth estimates for various sites (grouped by ocean basin; blue = Pacific Ocean, orange = Indian Ocean, green = Caribbean) used by the original authors. Different coral growth forms are indicated by text in brackets.

Radiocarbon. Regional deviations from the global offset between the atmosphere and the surface mixed layer (i.e., the marine reservoir effect) are dealt with using an offset (ΔR) during calibration, with ΔR often assumed to be constant through time. The resulting final calibrated probability distribution of the sample therefore includes the uncertainty in the construction of the marine calibration curve (currently Marine13⁵³), but not the uncertainty in the variation in ΔR through time⁵⁷. The effect on resulting calibrated age of: (i) spatially and temporally variation of the regional marine reservoir correction (ΔR) and; (ii) the effect of assuming a uniform, rather the Gaussian distribution for ΔR is explored further here. The examples provided are for illustrative purposes only.

In order to investigate the possible magnitude of this effect—i.e., potentially disparate modern and glacial values of ΔR for the same region—we explore the effect of using different values for ΔR , different error

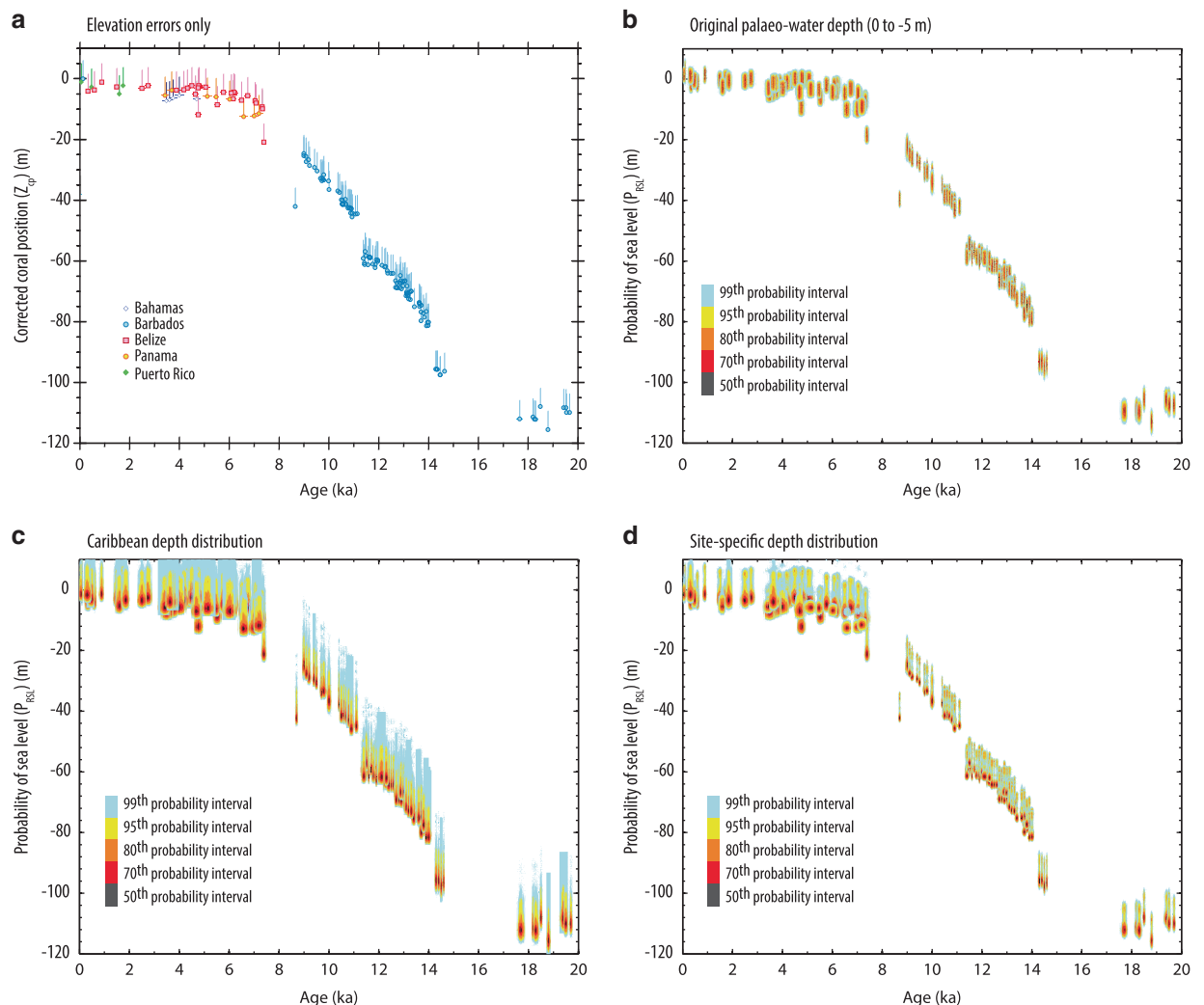


Figure 9. An example from the Caribbean (using the species *Acropora palmata*) of the effect of using different palaeo-water depth relationships on the resulting sea-level reconstructions. (a) the elevation uncertainties for the fossil *A. palmata* data; (b) the reconstructed sea level assuming a uniform distribution and a palaeo-water depth of 0 to 5 m; (c) the reconstructed sea level using our OBIS derived, ‘global’ species specific depth distribution and; (d) the reconstructed sea level using our regional depth distributions. P_{RSL} is reconstructed using a Monte-Carlo simulation of samples; coloured shading indicated the 99th (pale blue), 95th (yellow), 80th (orange), 70th (red) and 50th (black) percent probability intervals. This example is for illustrative purposes only and is not intended as a reinterpretation of the Caribbean *A. palmata* dataset.

distributions for ΔR (Gaussian and uniform distributions) for a marine dataset that possesses both radiocarbon and U-series age determinations (corals from Barbados^{82,83}). The calibrated ages (calibrated using the OxCal calibration software, version 4.3 (ref. 52).) are compared to the U-series dates for the same samples (recalculated assuming a closed system and the decay constants of²⁹) (Fig. 7). Note, this exercise is an example only; for sea-level reconstructions, we would use U-series ages in preference to radiocarbon ages for these samples, in order to negate both calibration issues and the unconstrained variable ΔR . Additionally, for this example, we assume that the U-series ages for the samples are reliable, i.e., that there has been no addition or loss of isotopes from the system (i.e., no open system behaviour) and negligible diagenetic alteration.

We recalibrate the radiocarbon ages using the following ΔR values: (i) those used by the original authors ($R = 400$ years, therefore $\Delta R = -5$ years⁸²; $R = 365 \pm 60$ years, therefore $\Delta R = -40$ years⁸³); (ii) the values used by the original authors ± 100 year uncertainty (assuming a Gaussian distribution); (iii) the preindustrial ΔR estimated for the Caribbean⁵⁶ ($\Delta R = -27 \pm 11$ years, $n = 8$; note, there are currently no observations from Barbados in the online ΔR database⁵⁶); (iv) using model output values⁸⁴ (using an iterative approach of transient, 3-dimensional simulations) that suggest variations in ΔR of 200 and 900 years for the Caribbean during the last deglacial. We use the upper and lower limits of their simulations with an arbitrary uncertainty of 100 years (i.e., $\Delta R = 200 \pm 100$ years and $\Delta R = 900 \pm 100$ years) using both a Gaussian and uniform distribution during calibration. Finally, we recalibrate the ages using temporally varying estimates of ΔR

(derived from Butzin *et al.*⁸⁴). Few of the of the recalibrated ages match the U-series ages for the samples, although the calibrated ages using the authors original estimates, preindustrial ΔR and those with no ΔR applied, offer a reasonable first approximation (Fig. 7). Using the modelled deglacial values for the Caribbean does not improve the match, although a variable ΔR does approximate the U-series ages slightly better than either of the model extremes (using both the Gaussian and uniform distributions). In this example, we are fortunate that the samples also possess U-series ages but it does illustrate the magnitude of the effect that choices regarding the ΔR value may have on the resulting age. This effect would be most acute during time intervals such as the last deglaciation, as major reorganisations in ocean circulation (as well as variations in ^{14}C production and sequestration by the various reservoirs) are documented^{85–87}. The sites in the database (i.e., primarily mid to low latitudes) should mitigate the magnitude of these effects because the scale of the oceanic changes (and hence ΔR) at those latitudes is smaller than at the higher latitudes⁸⁸. The ‘distortion’ in age due to variations in ΔR is likely greater than the effects of uncertainties in both the tectonically corrected elevation (Z_{cp}) and reconstructions of sea level probability (P_{RSL}) for this interval of time, given the relatively low rates of both subsidence and uplift for most sites in the database, and the relatively young ages of the samples. The example illustrates the current difficulty in constraining ΔR through time. Therefore, we apply only the preindustrial estimates⁵⁶ for the marine fossils when recalibrating ages in the database. Refinements in both the age determinations and reconstructed sea-level probability (P_{RSL}) for radiocarbon-dated marine sea-level indicators could be achieved as more robust constraints on both the spatial and temporal variation in ΔR through time become available.

Coral depth distributions

We compare our ecologically derived depth distributions of modern corals to: (i) other estimates/observations of the maximum depth of coral species at both global^{89,90} and local geographic scales^{75,91–97} (Fig. 3) and; (ii) palaeo-water depth determinations of the original publications (Fig. 8). The median and 95% confidence limits derived compare favourably with both the global and regional (where available) modern observations of the maximum depth observed for most species (Fig. 3). This lends confidence that the use of our ecological depth distributions is reasonable and, that use of a modern-analogue approach provides a first-order approximation of the relationship between the elevation of the fossil coral and sea level at the time of formation.

The global, ecologically derived depth distributions also compare favourably with palaeo-water depth estimations, originally derived using a variety of methodologies (e.g., modern assemblage, coral diversity/distribution) and geographical scales (site-specific to ocean basin scale comparisons). Figure 8 illustrates for each of three commonly dated coral taxa our ecological depth distributions and the palaeo-water depths. The modern ‘global’ estimates broadly replicate the palaeo-water depths. However, our depth distributions are unlikely to capture the full complexity in species distribution and diversity observed in modern coral reefs, nor are they able to capture all details of the site-specific relationship between corals and sea level. Therefore, these ecological depth distributions should be considered as ‘maximum’, first-order approximations of the relationship between the elevation of the coral and sea level at the time of formation. The effect of using different depth distributions on reconstructed sea-level probability (P_{RSL}) is illustrated for fossil *Acropora palmata* using data from the Caribbean (i.e., using the sub-basin and regional depth distributions) (Fig. 9). Once the elevation uncertainties are combined with either the palaeo-water depth estimates (assuming a 0 to 5 m depth preference and a uniform distribution, Fig. 9b) or the taxon-specific depth distributions (Fig. 9c), the regional depth distributions (Fig. 9d) result in ‘tighter’ P_{RSL} estimates for Barbados than either the palaeo-water depth or the Caribbean sub-basin depth distribution. Therefore, using a well-constrained, regional ecological depth distribution offers some promise of refining the vertical precision of reconstructed sea levels, and allows past sea levels to be reconstructed for samples where no information is available to define the relationship between the elevation of the fossil coral and sea level at the time of formation. Modern site-specific assemblage studies (i.e., documenting modern reef biota, facies and environmental characteristics) provide perhaps the best description of this relationship but our ecologically derived depth distributions (i.e., where only taxa and depth occurrence is given) offer a reasonable first-order approximation. Users of the database are able to use either the authors’ original palaeo-water depth determinations or our taxon depth distributions (at the ‘global’ or regional scale, Data Citation 2).

Tectonic corrections

The only independent (i.e., not constrained using the fossil sea-level indicators themselves) tectonic corrections are those for Tahiti and Mururoa Atoll (both French Polynesia^{16–18}). Hence, we are unable, so far, to validate the uplift/subsidence terms used in the database. This remains one of the main outstanding issues that hindering reconstructions of past sea level.

Code availability

We make the code used to calculate P_{RSL} available as a separate text file (Data Citation 3). This contains significant modifications from that given as a supplement^{12,98} to incorporate a uniform facies formation depth distribution and non-Gaussian age uncertainties.

Usage Notes

This release comprises 4 files (details of the file formats are within the square brackets):

1. Database [tab delimited file; 'Data Citation 1']
2. Summary of treatment of all the datasets compiled [text file; 'SupplementaryData']
3. Empirically derived coral depth distributions used to reconstruct sea level [tab delimited table; 'Data Citation 2']
4. Code: calculation of P_{RSL} for both 'coral' and 'range' type vertical uncertainties, as well as U-series and radiocarbon ages [pdf of Matlab code file; 'Data Citation 3']

We welcome contributions from authors of additional or clarifying information. These will be incorporated into any subsequent iteration of the database. When using data in this compilation, the original data collector(s) as well as the data compiler(s) should be credited⁹⁹.

Users are welcome to use either the original authors' (included in the database, Data Citation 1) or our ecologically derived depth distributions (Data Citation 2) to relate the elevation of the coral and sea level at the time of formation. Both are included in the database release, in addition to the code for reconstructing P_{RSL} (Data Citation 3).

No attempt has been made to correct for U-series open system behaviour, nor do we screen for age reliability. The inclusion of all metadata enables users to determine their own appropriate age reliability screening criteria. For simplicity, we record only the 68%, 95% confidence intervals, mean and sigma of the calibrated radiocarbon output. Again, the inclusion of all data and metadata relating to each radiocarbon determination enables users to both replicate our outputs and adapt the input into calibration software, if so desired. We do not attempt to account for temporal variations in ΔR .

The reconstructed P_{RSL} is a function of both eustatic and glacio-isostatic (GIA) processes. No correction has been made for GIA processes as this is outside the scope of this study.

References

1. Braconnot, P. *et al.* Evaluation of climate models using palaeoclimatic data. *Nat. Clim. Chang* **2**, 417–424 (2012).
2. Harrison, S. P. *et al.* Climate model benchmarking with glacial and mid-Holocene climates. *Clim. Dyn* **43**, 671–688 (2014).
3. Harrison, S. P. *et al.* Evaluation of CMIP5 palaeo-simulations to improve climate projections. *Nat. Clim. Chang* **5**, 735–743 (2015).
4. Schmidt, G. A. *et al.* Using palaeo-climate comparisons to constrain future projections in CMIP5. *Clim. Past* **10**, 221–250 (2014).
5. Church, J. A. *et al.* Sea Level Change. in *Climate Change 2013: The Physical Science Basis. Contribution of Working Group I to the Fifth Assessment Report of the Intergovernmental Panel on Climate Change* (eds. Stocker, T. F. *et al.*) 1137–1216 (Cambridge University Press, 2013).
6. Rohling, E. J., Haigh, I. D., Foster, G. L., Roberts, A. P. & Grant, K. M. A geological perspective on potential future sea-level rise. *Sci. Rep* **3**, 3461 (2013).
7. Rohling, E. J. *et al.* Sea-level and deep-sea-temperature variability over the past 5.3 million years. *Nature* **508**, 477–482 (2014).
8. DeConto, R. M. & Pollard, D. Contribution of Antarctica to past and future sea-level rise. *Nature* **531**, 591–597 (2016).
9. Shennan, I. & Horton, B. P. Holocene land- and sea-level changes in Great Britain. *J. Quat. Sci* **17**, 511–526 (2002).
10. Engelhart, S. E. & Horton, B. P. Holocene sea level database for the Atlantic coast of the United States. *Quat. Sci. Rev.* **54**, 12–25 (2012).
11. Khan, N. S. *et al.* Drivers of Holocene sea-level change in the Caribbean. *Quat. Sci. Rev.* **155**, 13–36 (2017).
12. Hibbert, F. D. *et al.* Coral indicators of past sea-level change: A global repository of U-series dated benchmarks. *Quat. Sci. Rev.* **145**, 1–56 (2016).
13. van de Plassche, O. Introduction. in *Sea-level Research: A Manual for the Collection and Evaluation of Data*, (ed. van de Plassche O.) 1–26 (Geo Books, 1986).
14. Shennan, I. Flandrian sea-level changes in the Fenland. II: Tendencies of sea-level movement, altitudinal changes, and local and regional factors. *J. Quat. Sci* **1**, 155–179 (1986).
15. Shennan, I., Long, A. J. & Horton, B. P. *Handbook of sea-level research*. (John Wiley and Sons Ltd., 2015).
16. Le Roy, I. *Evolution des volcans en système de point chaud: île de Tahiti, Archipel de la Société (Polynésie Française)*. (University of Paris, 1994).
17. Bard, E. *et al.* Deglacial sea level record from Tahiti corals and the timing of global meltwater discharge. *Nature* **382**, 241–244 (1996).
18. Trichet, J., Repellin, P. & Oustrière, P. Stratigraphy and subsidence of the Mururoa atoll (French Polynesia). *Mar. Geol.* **56**, 241–257 (1984).
19. Camoin, G. F., Ebren, P., Eisenhauer, A., Bard, E. & Faure, G. A 300 000-yr coral reef record of sea level changes, Mururoa atoll (Tuamotu archipelago, French Polynesia). *Palaeogeogr. Palaeoclimatol. Palaeoecol.* **175**, 325–341 (2001).
20. Bard, E., Hamelin, B. & Delanghe-Sabatier, D. Deglacial Meltwater Pulse 1B and Younger Dryas sea levels revisited with boreholes at Tahiti. *Science* **327**, 1235–1238 (2010).
21. Deschamps, P. *et al.* Ice-sheet collapse and sea-level rise at the Bølling warming 14,600 years ago. *Nature* **483**, 559–564 (2012).
22. Törnqvist, T. E. *et al.* Deciphering Holocene sea-level history on the U.S. Gulf Coast: a high-resolution record from the Mississippi Delta. *Bull. Geol. Soc. Am* **116**, 1026–1039 (2004).
23. Edwards, R. L., Gallup, C. D. & Cheng, H. Uranium-series dating of marine and lacustrine carbonates. *Rev. Mineral. Geochemistry* **52**, 363–405 (2003).
24. Stirling, C. H. & Andersen, M. B. Uranium-series dating of fossil coral reefs: extending the sea-level record beyond the last glacial cycle. *Earth Planet. Sci. Lett.* **284**, 269–283 (2009).
25. Dutton, A. Uranium-thorium dating. in *Handbook of Sea-Level Research* (eds Shennan I., Long A. J. & Horton B. P.) 386 (John Wiley and Sons Ltd., 2015).
26. Libby, W. F., Anderson, E. C. & Arnold, J. R. Age determination by radiocarbon content: world-wide assay of natural radiocarbon. *Science* **109**, 227–228 (1949).
27. Stuiver, M. & Suess, H. E. On the relationship between radiocarbon dates and true sample ages. *Radiocarbon* **8**, 534–540 (1966).
28. Guilderson, T. P., Reimer, P. J. & Brown, T. A. The boon and bane of radiocarbon dating. *Science* **307**, 362–364 (2005).
29. Cheng, H. *et al.* Improvements in ^{230}Th dating, ^{230}Th and ^{234}U half-life values, and U-Th isotopic measurements by multi-collector inductively coupled plasma mass spectrometry. *Earth Planet. Sci. Lett.* **371–372**, 82–91 (2013).
30. Ludwig, K. R. Isoplot: a geochronological toolkit for Microsoft Excel (2003).
31. Cheng, H. *et al.* The half-lives of uranium-234 and thorium-230. *Chem. Geol.* **169**, 17–33 (2000).

32. Stuiver, M., Reimer, P. J. & Reimer, R. W. $\delta^{13}\text{C}$ correction spreadsheet CALIB 7.1 (2018).
33. Stuiver, M. & Polach, H. A. Reporting of ^{14}C data. *Radiocarbon* **19**, 355–363 (1977).
34. Mook, W. G. & van der Plicht, J. Reporting ^{14}C activities and concentrations. *Radiocarbon* **41**, 227–239 (1999).
35. Millard, A. Conventions for reporting radiocarbon determinations. *Radiocarbon* **56**, 555–559 (2014).
36. Hogg, A. G. & Higham, T. F. G. ^{14}C dating of modern marine and estuarine shellfish. *Radiocarbon* **40**, 975–984 (1998).
37. Ulm, S. Marine and estuarine reservoir effects in central Queensland, Australia: determination of ΔR values. *Geoarchaeology - An Int. J.* **17**, 319–348 (2002).
38. Culleton, B. J. Implications of a freshwater radiocarbon reservoir correction for the timing of late Holocene settlement of the Elk Hills, Kern County, California. *J. Archaeol. Sci.* **33**, 1331–1339 (2006).
39. Reimer, P. J. Marine or estuarine radiocarbon reservoir corrections for mollusks? A case study from a medieval site in the south of England. *J. Archaeol. Sci.* **49**, 142–146 (2014).
40. De Vries, H. Variation in concentration of radiocarbon with time and location on Earth. *Proc. K. Ned. Akad. van Wet. Ser. B* **61**, 94–102 (1958).
41. Parnell, A. C., Buck, C. E. & Doan, T. K. A review of statistical chronology models for high-resolution, proxy-based Holocene palaeoenvironmental reconstruction. *Quat. Sci. Rev.* **30**, 2948–2960 (2011).
42. Trachsel, M. & Telford, R. J. All age-depth models are wrong, but are getting better. *The Holocene* **27**, 860–869 (2016).
43. Stuiver, M. & Reimer, P. J. Histograms obtained from computerized radiocarbon age calibration. *Radiocarbon* **31**, 817–823 (1989).
44. Michczyński, A. Is it possible to find a good point estimate of a calibrated radiocarbon date? *Radiocarbon* **49**, 393–401 (2007).
45. Weninger, B., Clare, L., Jöris, O., Jung, R. & Edinborough, K. Quantum theory of radiocarbon calibration. *World Archaeol.* **47**, 543–566 (2015).
46. Törnqvist, T. E. & Bierkens, M. F. P. How smooth should curves be for calibrating radiocarbon dates? *Radiocarbon* **36**, 11–26 (1994).
47. Weninger, B., Edinborough, K., Clare, L. & Jöris, O. Concepts of probability in radiocarbon analysis. *Doc. Praehist.* **38**, 1–20 (2011).
48. Michczyński, A. Influence of ^{14}C concentration changes in the past on statistical inference of time intervals. *Radiocarbon* **46**, 997–1004 (2004).
49. Ramsey, C. B. Deposition models for chronological records. *Quat. Sci. Rev.* **27**, 42–60 (2008).
50. Haslett, J. & Parnell, A. C. A simple monotone process with application to radiocarbon-dated depth chronologies. *J. R. Stat. Soc. Ser. C Appl. Stat.* **57**, 399–418 (2008).
51. Blaauw, M. & Christen, J. A. Flexible paleoclimate age-depth models using an autoregressive gamma process. *Bayesian Anal.* **6**, 457–474 (2011).
52. Bronk Ramsey, C. Bayesian Analysis of Radiocarbon Dates. *Radiocarbon* **51**, 337–360 (2009).
53. Reimer, P. J. *et al.* IntCal13 and Marine13 radiocarbon age calibration curves 0–50,000 years cal BP. *Radiocarbon* **55**, 1869–1887 (2013).
54. Hogg, A. G. *et al.* ShCal13 Southern Hemisphere Calibration, 0–50,000 Years Cal BP. *Radiocarbon* **55**, 1889–1903 (2012).
55. Stuiver, M. & Braziunas, T. F. Modeling atmospheric ^{14}C influences and ^{14}C ages of marine samples to 10,000 BC. *Radiocarbon* **35**, 137–189 (1993).
56. Reimer, P. J. & Reimer, R. W. Marine reservoir correction database (2018).
57. Reimer, R. W. & Reimer, P. J. An online application for ΔR calculation. *Radiocarbon* **13**, 1–5 (2016).
58. Stuiver, M., Pearson, G. W. & Braziunas, T. F. Radiocarbon age calibration of marine samples back to 9000 cal yr BP. *Radiocarbon* **28**, 980–1021 (1986).
59. Ascough, P., Cook, G. & Dugmore, A. Methodological approaches to determining the marine radiocarbon reservoir effect. *Prog. Phys. Geogr.* **29**, 532–547 (2005).
60. Olsen, J., Rasmussen, P. & Heinemeier, J. Holocene temporal and spatial variation in the radiocarbon reservoir age of three Danish fjords. *Boreas* **38**, 458–470 (2009).
61. Hughen, K. A. *et al.* Marine04 marine radiocarbon age calibration, 0–26 cal kyr BP. *Radiocarbon* **46**, 1029–1058 (2004).
62. Telford, R. J., Heegaard, E. & Birks, H. J. B. All age-depth models are wrong: but how badly? *Quat. Sci. Rev.* **23**, 1–5 (2004).
63. Shennan, I. Interpretation of Flandrian sea-level data from the Fenland, England. *Proc. Geol. Assoc.* **93**, 53–63 (1982).
64. Veron, J. E. N. *Corals in space and time. The biogeography and evolution of the Scleractinia.* (University of New South Wales Press, 1995).
65. Veron, J. E. N. *et al.* Delineating the Coral Triangle. *Galaxea, J. Coral Reef Stud.* **11**, 91–100 (2009).
66. Done, T. J. Patterns in the distribution of coral communities across the central Great Barrier Reef. *Coral Reefs* **1**, 95–107 (1982).
67. Veron, J. E. N. *Corals of the world.* (Australian Institute of Marine Science, 2000).
68. DeVantier, L. M., De'ath, G., Turak, E., Done, T. J. & Fabricius, K. E. Species richness and community structure of reef-building corals on the nearshore Great Barrier Reef. *Coral Reefs* **25**, 329–340 (2006).
69. Veron, J. E. N. Checklist of the hermatypic corals of Vanuatu. *Pacific Sci.* **44**, 51–70 (1990).
70. Pandolfi, J. M. *et al.* Global trajectories of the long-term decline of coral reef ecosystems. *Science* **301**, 955–958 (2003).
71. Gardner, T. A., Cote, I. M., Gill, J. A., Grant, A. & Watkinson, A. R. Long-term region-wide declines in Caribbean corals. *Science* **301**, 958–960 (2003).
72. Pandolfi, J. M. Coral community dynamics at multiple scales. *Coral Reefs* **21**, 13–23 (2002).
73. Jackson, J. B. C. Pleistocene perspectives on coral reef community structure. *Am. Zool.* **32**, 719–731 (1992).
74. Goreau, T. F. The ecology of Jamaican coral reefs I. Species composition and zonation. *Ecology* **40**, 67–90 (1959).
75. Goreau, T. F. & Wells, J. W. The shallow-water scleractinian of Jamaica: revised list of species and their vertical distribution range. *Bull. Mar. Sci.* **17**, 442–453 (1967).
76. Mesolella, K. J. *The uplifted reefs of Barbados: physical stratigraphy, facies relationships and absolute chronology.* (Brown University, 1968).
77. Stearn, C. W., Scoffin, T. P. & Martindale, W. Calcium carbonate budget of a fringing reef on the west coast of Barbados. Part I - Zonation and productivity. *Bull. Mar. Sci.* **27**, 479–510 (1977).
78. Scoffin, T. P. Coral reefs. *Coral Reefs* **11**, 57–77 (1992).
79. Scoffin, T. P. *et al.* Calcium carbonate budget of a fringing reef on the west coast of Barbados: Part II - Erosion, sediments and internal structure. *Bull. Mar. Sci.* **302**, 457–508 (1980).
80. Pandolfi, J. M. & Minchin, P. A comparison of taxonomic composition and diversity between reef coral life and death assemblages in Madang Lagoon, Papua New Guinea. *Palaeogeogr. Palaeoclimatol. Palaeoecol.* **119**, 321–341 (1995).
81. Greenstein, B. J. & Pandolfi, J. M. Taphonomic alteration of reef corals: effects of reef environment and coral growth form. II. The Great Barrier Reef. *Palaios* **18**, 495–509 (2003).
82. Bard, E., Hamelin, B., Fairbanks, R. G. & Zindler, A. Calibration of the ^{14}C timescale over the past 30,000 years using mass spectrometric U–Th ages from Barbados corals. *Nature* **345**, 405–410 (1990).

83. Fairbanks, R. G. *et al.* Radiocarbon calibration curve spanning 0 to 50,000 years BP based on paired $^{230}\text{Th}/^{234}\text{U}/^{238}\text{U}$ and ^{14}C dates on pristine corals. *Quat. Sci. Rev.* **24**, 1781–1796 (2005).
84. Butzin, M., Prange, M. & Lohmann, G. Readjustment of glacial radiocarbon chronologies by self-consistent three-dimensional ocean circulation modeling. *Earth Planet. Sci. Lett.* **317–318**, 177–184 (2012).
85. Hughen, K. A. *et al.* ^{14}C activity and global carbon cycle changes over the past 50,000 years. *Science* **303**, 202–207 (2004).
86. Muscheler, R. *et al.* Changes in the carbon cycle during the last deglaciation as indicated by the comparison of ^{10}Be and ^{14}C records. *Earth Planet. Sci. Lett.* **219**, 325–340 (2004).
87. Schmittner, A. & Galbraith, E. D. Glacial greenhouse-gas fluctuations controlled by ocean circulation changes. *Nature* **456**, 373–376 (2008).
88. Singarayer, J. S. *et al.* An oceanic origin for the increase of atmospheric radiocarbon during the Younger Dryas. *Geophys. Res. Lett.* **35**, 1–6 (2008).
89. Carpenter, K. *et al.* One-third of reef-building corals face elevated extinction risk from climate change and local impacts. *Science* **321**, 560–563 (2008).
90. Muir, P. R., Wallace, C. C., Done, T. & Aguirre, J. D. Limited scope for latitudinal extension of reef corals. *Science* **348**, 1135–1138 (2015).
91. Bouchon, C. Quantitative study of the scleractinian coral communities of a fringing reef of Reunion Island (Indian Ocean). *Mar. Ecol. Prog. Ser.* **4**, 273–288 (1981).
92. Kühlmann, D. H. H. Composition and ecology of deep-water coral associations. *Helgoländer Meeresuntersuchungen* **36**, 183–204 (1983).
93. Titlyanov, E. A. & Latypov, Y. Y. Coral Reefs in the sublittoral zone of South China Sea Islands. *Coral Reefs* **10**, 133–138 (1991).
94. Bongaerts, P. *et al.* Mesophotic coral ecosystems on the walls of Coral Sea atolls. *Coral Reefs* **30**, 335–335 (2011).
95. Bridge, T. C. L. *et al.* Diversity of Scleractinia and Octocorallia in the mesophotic zone of the Great Barrier Reef, Australia. *Coral Reefs* **31**, 179–189 (2012).
96. Wagner, D. *et al.* Mesophotic surveys of the flora and fauna at Johnston Atoll, Central Pacific Ocean. *Mar. Biodivers. Rec.* **7**, 1–10 (2014).
97. Eyal, G. *et al.* Spectral diversity and regulation of coral fluorescence in a mesophotic reef habitat in the Red Sea. *PLoS One* **10**, 1–19 (2015).
98. Williams, F. H. *A geophysical approach to reconstructing past global mean sea levels using highly resolved sea-level records.* (University of Southampton, 2016).
99. Düsterhus, A. *et al.* Palaeo-sea-level and palaeo-ice-sheet databases: problems, strategies, and perspectives. *Clim. Past* **12**, 911–921 (2016).
100. De Deckker, P. & Yokoyama, Y. Micropalaeontological evidence for Late Quaternary sea-level changes in Bonaparte Gulf, Australia. *Glob. Planet. Change* **66**, 85–92 (2009).
101. Ishiwa, T. *et al.* Reappraisal of sea-level lowstand during the Last Glacial Maximum observed in the Bonaparte Gulf sediments, northwestern Australia. *Quat. Int.* **397**, 373–379 (2016).
102. Nicholas, W. A. *et al.* Pockmark development in the Petrel Sub-basin, Timor Sea, Northern Australia: seabed habitat mapping in support of CO₂ storage assessments. *Cont. Shelf Res.* **83**, 129–142 (2014).
103. Yokoyama, Y., Lambeck, K., De Deckker, P., Johnston, P. & Fifield, L. K. Timing of the Last Glacial Maximum from observed sea-level minima. *Nature* **406**, 713–716 (2000).
104. Yokoyama, Y., De Deckker, P., Lambeck, K., Johnston, P. & Fifield, L. K. Sea-level at the Last Glacial Maximum: evidence from northwestern Australia to constrain ice volumes for Oxygen Isotope Stage 2. *Palaeogeogr. Palaeoclimatol. Palaeoecol.* **165**, 281–297 (2001).
105. Jongsma, D. Eustatic sea level changes in the Arafura Sea. *Nature* **228**, 150–151 (1970).
106. Thom, B. G. & Chappell, J. Holocene sea levels relative to Australia. *Search* **6**, 90–93 (1975).
107. Ferland, M. A., Roy, P. S. & Murray-Wallace, C. V. Glacial lowstand deposits on the outer continental shelf of southeastern Australia. *Quat. Res.* **44**, 294–299 (1995).
108. Gill, E. D. Quaternary shorelines research in Australia and New Zealand. *Aust. J. Earth Sci.* **31**, 106–111 (1967).
109. Shepard, M. J. *Coastal geomorphology of the Myall Lakes Area, NSW.* (University of Sydney, 1970).
110. Switzer, A. D., Sloss, C. R., Jones, B. G. & Bristow, C. S. Geomorphic evidence for mid-late Holocene higher sea level from southeastern Australia. *Quat. Int.* **221**, 13–22 (2010).
111. Thom, B. G., Hails, J. R. & Martin, A. R. H. Radiocarbon evidence against higher postglacial sea levels in eastern Australia. *Mar. Geol.* **7**, 161–168 (1969).
112. Belperio, A. P., Hails, J. R. & Gostin, V. A. A review of Holocene sea levels in South Australia. in *Australian Sea Levels in the Last 15,000 Years: A Review*, (ed. Hopley, D.) 37–47 (James Cook University of North Queensland, 1983).
113. Belperio, A. P., Hails, J. R., Gostin, V. A. & Polach, H. A. The stratigraphy of coastal carbonate banks and Holocene sea levels of northern Spencer Gulf, South Australia. *Mar. Geol.* **61**, 297–313 (1984).
114. Belperio, A. P. Land subsidence and sea level rise in the Port Adelaide estuary: Implications for monitoring the greenhouse effect. *Aust. J. Earth Sci.* **40**, 359–368 (1993).
115. Belperio, A. P., Harvey, N. & Bourman, R. P. Spatial and temporal variability in the Holocene sea-level record of the South Australian coastline. *Sediment. Geol.* **150**, 153–169 (2002).
116. Burne, R. V. Relative fall of Holocene sea level and coastal progradation, northeastern Spencer Gulf, South Australia. *BMR J. Aust. Geol. Geophys.* **7**, 35–45 (1982).
117. Harvey, N., Barnett, E. J., Bourman, R. P. & Belperio, A. P. Holocene sea-level change at Port Pirie, South Australia: a contribution to global sea-level rise estimates from tide gauges. *J. Coast. Res.* **1**, 607–615 (1999).
118. Short, A. D., Fotheringham, D. G. & Buckley, R. C. *Coastal morphodynamics and Holocene evolution of the Eyre Peninsula coast, South Australia. Coastal Studies Unit Technical Report 86/2.* (University of Sydney, 1986).
119. Gill, E. D. & Hopley, D. Holocene sea levels in eastern Australia— a discussion. *Mar. Geol.* **12**, 223–233 (1972).
120. Beaman, R., Larcombe, P. & Carter, R. M. New evidence for the Holocene sea-level high from the Inner Shelf, central Great Barrier Reef, Australia. *SEPM J. Sediment. Res.* **64A**, 881–885 (1994).
121. Belperio, A. P. Negative evidence for a mid-Holocene high sea level along the coastal plain of the Great Barrier Reef Province. *Mar. Geol.* **32**, 1–9 (1979).
122. Carter, R. M., Johnson, D. P. & Hooper, K. G. Episodic post-glacial sea-level rise and the sedimentary evolution of a tropical continental embayment (Cleveland Bay, Great Barrier Reef shelf, Australia). *Aust. J. Earth Sci.* **40**, 229–255 (1993).
123. Woodroffe, S. A. Testing models of mid to late Holocene sea-level change, North Queensland, Australia. *Quat. Sci. Rev.* **28**, 2474–2488 (2009).
124. Chappell, J., Chivas, A., Wallensky, E., Polach, H. A. & Aharon, P. Holocene palaeo-environmental changes, central to northern Great Barrier Reef inner zone. *AGSO J. Aust. Geol. Geophys.* **8**, 223–235 (1983).
125. Grindrod, J. & Rhodes, E. G. Holocene sea-level history of a tropical estuary: Missionary Bay, North Queensland in *Coastal Geomorphology in Australia* (ed. Thom B. G.) 151–178 (Academic Press, 1984).

126. Harvey, N., Belperio, A. P., Bourman, R. P., James, K. & Brunskill, G. New evidence contributing to the debate on the Holocene high sea-level stand in north east Queensland, Australia. *Third Joint Conference of the New Zealand Geographical Society and the Institute of Australian Geographers* (eds Holland P., Stephenson F. & Wearing A.) 177–184 (New Zealand Geographical Society, 2001).
127. Horton, B. P. *et al.* Reconstructing Holocene sea-level change for the Central Great Barrier Reef (Australia) using subtidal foraminifera. *J. Foraminifer. Res.* **37**, 47–63 (2007).
128. Kench, P. S., Smithers, S. G. & McLean, R. F. Rapid reef island formation and stability over an emerging reef flat: Bewick cay, northern Great Barrier Reef, Australia. *Geology* **40**, 347–350 (2012).
129. Larcombe, P. & Carter, R. M. Sequence architecture during the Holocene transgression: an example from the Great Barrier Reef shelf, Australia. *Sediment. Geol.* **117**, 97–121 (1998).
130. Larcombe, P., Carter, R. M., Dye, J., Gagan, M. K. & Johnson, D. P. New evidence for episodic post-glacial sea-level rise, central Great Barrier Reef, Australia. *Mar. Geol.* **127**, 1–44 (1995).
131. Leonard, N. D. *et al.* Holocene sea level instability in the southern Great Barrier Reef, Australia: high-precision U–Th dating of fossil microatolls. *Coral Reefs* **35**, 625–639 (2016).
132. Lewis, S. E., Wüst, R. A. J., Webster, J. M. & Shields, G. A. Mid-late Holocene sea-level variability in eastern Australia. *Terra Nov* **20**, 74–81 (2008).
133. Lewis, S. E. *et al.* Development of an inshore fringing coral reef using textural, compositional and stratigraphic data from Magnetic Island, Great Barrier Reef, Australia. *Mar. Geol.* **299–302**, 18–32 (2012).
134. Lewis, S. E. *et al.* Rapid relative sea-level fall along north-eastern Australia between 1200 and 800 cal. yr BP: An appraisal of the oyster evidence. *Mar. Geol.* **370**, 20–30 (2015).
135. Ohlenbusch, R. *Post-glacial sequence stratigraphy and sedimentary development of the continental shelf off Townsville, Central Great Barrier Reef Province*. (James Cook University, 1991).
136. Spenceley, A. P. *The geomorphological and zonal development of mangrove swamps in the Townsville Area*. (North Queensland: James Cook University, 1980).
137. Tye, S. *A stratigraphic and geochemical study of the Holocene evolution of Southern Halifax Bay*. (North Queensland: James Cook University, 1992).
138. Veeh, H. H. & Veevers, J. J. Sea level at -175 m off the Great Barrier Reef 13,600 to 17,000 year ago. *Nature* **226**, 536–537 (1970).
139. Yu, K.-F. & Zhao, J. U-series dates of Great Barrier Reef corals suggest at least +0.7 m sea level ~7000 years ago. *The Holocene* **20**, 161–168 (2010).
140. Woodroffe, C. D., Kennedy, D. M., Hopley, D., Rasmussen, C. E. & Smithers, S. G. Holocene reef growth in Torres Strait. *Mar. Geol.* **170**, 331–346 (2000).
141. Ota, Y., Berryman, K. R., Hull, A. G., Miyauchi, T. & Iso, N. Age and height distribution of holocene transgressive deposits in eastern North Island, New Zealand. *Palaeogeogr. Palaeoclimatol. Palaeoecol.* **68**, 135–151 (1988).
142. Gibb, J. G. A New Zealand regional Holocene eustatic sea-level curve and its application to determination of vertical tectonic movements. *R. Soc. New Zeal. Bull.* **24**, 377–395 (1986).
143. Gibb, J. G. *Late Quaternary shoreline movements in New Zealand*. (Victoria University of Wellington, 1979).
144. Leach, B. F. The terminal age for the Lower Wairarapa estuarine environment. *J. R. Soc. New Zeal.* **14**, 207–298 (1984).
145. Leach, B. F. & Anderson, A. J. The transformation from an estuarine to lacustrine environment in the lower Wairarapa. *J. R. Soc. New Zeal.* **4**, 267–275 (1974).
146. McFagden, B. G. Age relationship between a Maori plaggen soil and Moa-hunter sites on the west Wellington coast. *New Zeal. J. Geol. Geophys.* **23**, 249–256 (1980).
147. Mildenhall, D. C. Holocene pollen diagrams from Pauatahanui Inlet, Porirua, New Zealand. *New Zeal. J. Geol. Geophys.* **22**, 585–591 (1979).
148. Ota, Y. *et al.* Holocene marine terraces in the northeastern coast of North Island, New Zealand. in *International Symposium Coastal Evolution in Holocene* 109–112 (Ministry for Education, Science and Culture, 1983).
149. Ota, Y., Hull, A. G. & Berryman, K. R. Coseismic uplift of Holocene marine terraces in the Pakarua River Area, eastern North Island, New Zealand. *Quat. Res.* **35**, 331–346 (1991).
150. Schofield, J. C. Sea level fluctuations during the last 4,000 years as recorded by a chenier plain, Firth of Thames, New Zealand. *New Zeal. J. Geol. Geophys.* **3**, 467–485 (1960).
151. Singh, L. J. Uplift and tilting of the Oterei coast, Wairarapa, New Zealand, during the last ten thousand years. *R. Soc. New Zeal. Bull.* **9**, 217–219 (1971).
152. Woodroffe, C. D., Curtis, R. J. & McLean, R. F. Development of a chenier plain, Firth of Thames, New Zealand. *Mar. Geol.* **53**, 1–22 (1983).
153. Yoshikawa, T., Ota, Y., Yonekura, N., Okada, A. & Nozomi, I. S. O. Marine terraces and their tectonic deformation on the northeast coast of the North Island, New Zealand. *Geogr. Rev. Jpn.* **53**, 238–262 (1980).
154. Brown, L. J. Sheet S76-Kaiapoi. Geological Map of New Zealand 1. 63360 (1973).
155. Suggate, R. P. Post-glacial sea-level rise in the Christchurch metropolitan area, New Zealand. *Geol. En Mijnb.* **47**, 291–297 (1968).
156. Pirazzoli, P. A. & Montaggioni, L. F. Holocene sea-level changes in French Polynesia. *Palaeogeogr. Palaeoclimatol. Palaeoecol.* **68**, 153–175 (1988).
157. Pirazzoli, P. A. A reconnaissance and survey of Temoe Atoll (South Pacific Ocean). *J. Coast. Res.* **3**, 307–322 (1987).
158. Pirazzoli, P. A., Delibrias, G., Montaggioni, L. F., Saliege, J. F. & Vergnaud-Grazzini, C. Vitesse de croissance latérale des platiers et évolution morphologique récente de l'atoll de Reao, îles Tuamotu, Polynésie française. *Ann. l'Institut Océanographique* **63**, 57–68 (1987).
159. Pirazzoli, P. A. & Montaggioni, L. F. Les îles Gambier et l'atoll de Temoe (Polynésie française) : anciennes lignes de rivage et comportement géodynamique. *Géodynamique* **2**, 13–25 (1987).
160. Chevalier, J. P. & Salvat, B. Etude géomorphologique de l'atoll fermé de Taïaro. *Cah. du Pacifique* **19**, 169–291 (1976).
161. Pirazzoli, P. A. *et al.* Leeward islands, Maupiti, Tupai, Bora Bora, Huahine, Society archipelago. *Proceedings of the Fifth International Coral Reef Congress, Tahiti, 27 May -1 June 1985* **1**, 17–72 (1985).
162. Salvat, B., Richard, G., Poli, G., Chevalier, J. P. & Bagnis, R. Geomorphology and biology of Taiari Atoll, Tuamotu Archipelago. in *Proceedings of the Third International Coral Reef Congress* (ed. Taylor D. L.) 289–296 (University of Miami, 1977).
163. Delibrias, G., Guillier, M. T. & Labeyrie, J. Gif natural radiocarbon measurements VIII. *Radiocarbon* **16**, 15–94 (1974).
164. Montaggioni, L. F. Makatea Island, Tuamotu Archipelago. in *Proceeding of the Fifth International Coral Reef Congress, Tahiti* (eds. Delesalle, B., Galzin, R. & Salvat, B.) 103–158 (1985).
165. Pirazzoli, P. A. Bathymetric mapping of coral reefs and atolls from satellite. in *Proceedings of the Fifth International Coral Reef Congress, Tahiti* (eds. Gabriele, C. & Harmelin, M.) 539–599 (1985).
166. Pirazzoli, P. A. & Montaggioni, L. F. Variations récentes du niveau de l'océan et du bilan hydrologique dans l'atoll de Takapoto (Polynésie Française). *Comptes rendus l'Académie des Sci. Série 2, Mécanique, Phys. Chim. Sci. l'univers, Sci. la Terre* **299**, 321–326 (1984).

167. Pirazzoli, P. A. & Montaggioni, L. F. Late Holocene sea-level changes in the northwest Tuamotu Islands, French Polynesia. *Quat. Res* **25**, 350–368 (1986).
168. Pirazzoli, P. A., Montaggioni, L. F., Vergnaud-Grazzini, C. & Saliege, J. F. Late Holocene sea levels and coral reef development in Vahitahi Atoll, eastern Tuamotu Islands, Pacific Ocean. *Mar. Geol* **76**, 105–116 (1987).
169. Pirazzoli, P. A., Koba, M., Montaggioni, L. F. & Person, A. Anaa (Tuamotu Islands, Central Pacific): an incipient rising atoll? *Mar. Geol* **82**, 261–269 (1988).
170. Pirazzoli, P. A., Montaggioni, L. F., Salvat, B. & Faure, G. Late Holocene sea level indicators from twelve atolls in the central and eastern Tuamotus (Pacific Ocean). *Coral Reefs* **7**, 57–68 (1988).
171. Allen, M. S. *et al.* Timing, magnitude and effects of late Holocene sea level drawdown on island habitability, Aitutaki, Cook Islands. *Archaeol. Ocean.* **51**, 108–121 (2016).
172. Goodwin, I. D. & Harvey, N. Subtropical sea-level history from coral microatolls in the Southern Cook Islands, since 300 AD. *Mar. Geol* **253**, 14–25 (2008).
173. Moriwaki, H., Chikamori, M., Okuno, M. & Nakamura, T. Holocene changes in sea level and coastal environments on Rarotonga, Cook Islands, South Pacific Ocean. *The Holocene* **16**, 839–848 (2006).
174. Yonekura, N. *et al.* Holocene fringing reefs and sea-level change in Mangaia Island, Southern Cook Islands. *Palaeogeogr. Palaeoclimatol. Palaeoecol* **68**, 177–188 (1988).
175. Guilderson, T. P., Burckle, L., Hemming, S. & Peltier, W. R. Late Pleistocene sea level variations derived from the Argentine Shelf. *Geochemistry Geophys. Geosystems* **1**, 1055 (2000).
176. Camoin, G. F. *et al.* Holocene sea level changes and reef growth in southwestern Indian ocean. *Coral Reefs* **16**, 247–259 (1997).
177. Colonna, M., Casanova, J., Dullo, W.-C. & Camoin, G. F. Sea-level changes and $\delta^{18}\text{O}$ record for the past 34,000 yr from Mayotte reef, Indian Ocean. *Quat. Res* **46**, 335–339 (1996).
178. Zinke, J. *et al.* Postglacial flooding history of Mayotte Lagoon (Comoro Archipelago, southwest Indian Ocean). *Mar. Geol* **194**, 181–196 (2003).
179. Montaggioni, L. F. & Faure, G. Response of reef coral communities to sea-level rise : a Holocene model from Mauritius (Western Indian Ocean). *Sedimentology* **44**, 1053–1070 (1997).
180. Gischler, E., Hudson, J. H. & Pisera, A. Late Quaternary reef growth and sea level in the Maldives (Indian Ocean). *Mar. Geol* **250**, 104–113 (2008).
181. Kench, P. S., McLean, R. F. & Nichol, S. L. New model of reef-island evolution: Maldives, Indian Ocean. *Geology* **33**, 145–148 (2005).
182. Kench, P. S., Smithers, S. G., McLean, R. F. & Nichol, S. L. Holocene reef growth in the Maldives: evidence of a mid-Holocene sea-level highstand in the central Indian Ocean. *Geology* **37**, 455–458 (2009).
183. Woodroffe, C. D. Morphology and evolution of reef islands in the Maldives. in *Proceedings of the Seventh International Coral Reef Symposium* (ed. Richmond, R. H.) **2**, 1217–1226 (University of Guam Press, 1993).
184. Woodroffe, S. A. *et al.* Radiocarbon dating of mangrove sediments to constrain Holocene relative sea-level change on Zanzibar in the southwest Indian Ocean. *The Holocene* **25**, 820–831 (2015).
185. Wiedicke, M., Kudrass, H. R. & Hübscher, C. Oolitic beach barriers of the last glacial sea-level lowstand at the outer Bengal shelf. *Mar. Geol* **157**, 7–18 (1999).
186. Banerjee, P. K. Holocene and Late Pleistocene relative sea level fluctuations along the east coast of India. *Mar. Geol* **167**, 243–260 (2000).
187. Katupotha, J. & Fujiwara, K. Holocene sea level change on the southwest and south coasts of Sri Lanka. *Palaeogeogr. Palaeoclimatol. Palaeoecol* **68**, 189–203 (1988).
188. Grobber, N. G., Mason, T. R. & Cooper, J. A. G. uMgababa Lagoon: pre- and post-flood sedimentology in *Sedimentation in estuaries and lagoons (S.E.A.L.)*. (Department of Geology and Applied Geology, University of Natal, 1988).
189. King, L. C. *The Natal Monocline: Explaining the Structure and Origin of Natal*. (University of Natal Press, 1972).
190. Maud, R. R. Quaternary geomorphology and soil formation in coastal Natal. *Zeitschrift für Geomorphol.* **7**, 155–199 (1968).
191. Ramsay, P. J. & Cooper, J. A. G. Late Quaternary sea-level change in South Africa. *Quat. Res* **57**, 82–90 (2002).
192. Miller, D. E., Yates, R. J., Jerardino, A. & Parkington, J. E. Late Holocene coastal change in the southwestern Cape, South Africa. *Quat. Int* **29/30**, 3–10 (1995).
193. Ramsay, P. J. *Sedimentology, coral reef zonation, and Late Pleistocene coastline models of the Sodwana Bay continental shelf, northern Zululand*. (University of Natal, 1991).
194. Ramsay, P. J. 9000 years of sea-level change along the southern African coastline. *Quat. Int* **31**, 71–75 (1996).
195. Ramsay, P. J. & Mason, T. R. Development of a type zoning scheme for Zululand coral reefs. *J. Coast. Res* **6**, 829–852 (1990).
196. Reddering, J. S. V. Evidence for a middle Holocene transgression, Keurbooms estuary, South Africa. *Palaeoecol. Africa* **19**, 79–87 (1988).
197. Siesser, W. G. Relict and recent beachrock from southern Africa. *Bull. Geol. Soc. Am* **85**, 1849–1854 (1974).
198. Vogel, J. C. & Marais, M. Pretoria radiocarbon dates I. *Radiocarbon* **13**, 378–394 (1971).
199. Vogel, J. C. & Visser, E. Pretoria radiocarbon dates II. *Radiocarbon* **23**, 43–80 (1981).
200. Yates, R. J. *et al.* A late mid-Holocene high sea level: A preliminary report of geoarchaeology at Elands Bay, western Cape Province, South Africa. *S. Afr. J. Sci.* **82**, 164–165 (1986).
201. Hanebuth, T. J. J., Statteger, Karl & Grootes, P. M. Rapid flooding of the Sunda shelf: a late glacial sea level record. *Science* **288**, 1033–1035 (2000).
202. Hanebuth, T. J. J., Statteger, K. & Bojanowski, A. Termination of the Last Glacial Maximum sea-level lowstand: the Sunda-Shelf data revisited. *Glob. Planet. Change* **66**, 76–84 (2009).
203. Tanabe, S., Tateishi, M. & Shibata, Y. The sea-level record of the last deglacial in the Shinano River incised-valley fill, Echigo Plain, central Japan. *Mar. Geol* **266**, 223–231 (2009).
204. Chen, Y. & Lui, T. Sea-level changes in the last several thousand years, Penghu Islands, Taiwan Strait. *Quat. Res* **45**, 254–262 (1996).
205. Chen, C., Huang, B. & Wang, M. The chronology of Holocene stratigraphy in Fujian coast. *Taiwan Strait* **1**, 64–73 (1982).
206. Dai, P. *Holocene peat formation of Mao-Dian-Liu region, southern Yangtze delta plain*. (East China Normal University: Shanghai, 1987).
207. Hong, X. Late Quaternary strata and its palaeogeographic significance of Hang-Jia-Hu plain. in *Geography* 224–231 (East China Normal University Press, 1990).
208. Huang, Z., Zhang, Z. & Zong, Y. Changes of sea level in south China coast since the Late Pleistocene. in *China Sea-level Changes* (ed. The IGCP 200 China Working Group) 178–194 (China Ocean Press, 1986).
209. Li, P., Qiao, P., Zheng, H., Fang, G. & Huang, G. *Environmental evolution of Zhujiang Delta in the past 10000 years* (China Ocean Press, 1991).
210. Sun, S. & Huang, Y. *Taihu Lake*. (China Ocean Press, 1993).
211. Wang, Z. The marine transgression of Zhejiang Province, China. in *Quaternary Coastline Changes in China* 143–156 (China Ocean Press, 1991).

212. Yang, D. Tidal-level changes in the Changjiang estuary during Holocene. in *Sea-level Changes* 143–156 (China Ocean Press, 1986).
213. Yim, W. W. S. Radiocarbon dates from Hong Kong and their geological implication. *J. Hong Kong Archaeol. Soc* **11**, 50–63 (1986).
214. Zhang, Z. & Lui, R. The Holocene stratigraphy of the coast of Hainan Island. *Geogr. Sci* **7**, 129–138 (1987).
215. Zhao, X. *China Sea-level Change*. (Shandong Scientific and Technological Press, 1996).
216. Zhu, C., Cheng, P., Lu, C. & Wang, W. Shoreline movements in the Yangtze delta and Su-bei coastal areas over the last 7000 years. *Sci. Geogr. Sin* **16**, 207–213 (1996).
217. Zong, Y. Postglacial stratigraphy and sea-level changes in the Han River Delta, China. *J. Coast. Res* **8**, 1–8 (1992).
218. Zong, Y. Mid-Holocene sea-level highstand along the Southeast Coast of China. *Quat. Int* **117**, 55–67 (2004).
219. Saito, Y. *et al.* Delta progradation and chenier formation in the Huanghe (Yellow River) delta, China. *J. Asian Earth Sci.* **18**, 489–497 (2000).
220. Liu, J. *et al.* Sedimentary record of environmental evolution off the Yangtze River estuary, East China Sea, during the last ~13,000 years, with special reference to the influence of the Yellow River on the Yangtze River delta during the last 600 years. *Quat. Sci. Rev.* **29**, 2424–2438 (2010).
221. Yu, K. F., Zhao, J. X., Done, T. & Chen, T. G. Microatoll record for large century-scale sea-level fluctuations in the mid-Holocene. *Quat. Res* **71**, 354–360 (2009).
222. Kim, J. M. & Kennett, J. P. Paleoenvironmental changes associated with the Holocene marine transgression, Yellow Sea (Hwanghae). *Mar. Micropaleontol.* **34**, 71–89 (1998).
223. Chaimanee, N., Tiaypirach, S. & Jongkanjanasoonthorn, Y. *Quaternary Geology of Satting Pra and Khao Chaison Areas*. (1985).
224. Horton, B. P. *et al.* Holocene sea levels and palaeoenvironments, Malay-Tahi Peninsula, southeast Asia. *Holocene* **8**, 1199–1213 (2005).
225. Scoffin, T. P. & Le Tissier, M. D. A. Late Holocene sea level and reef-flat progradation, Phuket, South Thailand. *Coral Reefs* **17**, 273–276 (1998).
226. Sinsakul, S. Evidence of Quaternary sea level changes in the coastal areas of Thailand: a review. *J. Southeast Asian Earth Sci* **7**, 23–37 (1992).
227. Somboon, J. R. P. & Thiramongkol, N. Holocene highstand shoreline of the Chao Phraya delta, Thailand. *J. Southeast Asian Earth Sci* **7**, 53–60 (1992).
228. Thiramongkol, N. Geomorphology of the lower Central Plain, Thailand. in *Proceedings of the 3rd meeting of the working group of river and coastal plain*, 103–117 (Chulalongkorn University, 1984).
229. Tiaypunte, S. & Theerarungsikul, N. *The geology of map sheet Amphoe Nongjik and Changwat Pattani*, Geological Survey Report. (1988).
230. Geyh, M. A., Streif, H. & Kudrass, H.-R. Sea-level changes during the late Pleistocene and Holocene in the Strait of Malacca. *Nature* **278**, 441–443 (1979).
231. Hassan, K. bin. *Holocene sea level changes in Kelang and Kuantan*. (Peninsular Malaysia: Durham University, 2001).
232. Tjia, H. D., Fujii, S. & Kigoshi, K. Holocene shorelines of Tioman Island in the South China Sea. *Geol. En Mijnb* **62**, 599–604 (1983).
233. Bird, M. I. *et al.* An inflection in the rate of early mid-Holocene eustatic sea-level rise: a new sea-level curve from Singapore. *Estuar. Coast. Shelf Sci.* **71**, 523–536 (2007).
234. Bird, M. I. *et al.* Punctuated eustatic sea-level rise in the early mid-Holocene. *Geology* **38**, 803–806 (2010).
235. Hesp, P. A., Hung, C. C., Hilton, M., Ming, C. L. & Turner, I. M. A first tentative Holocene sea-level curve for Singapore. *J. Coast. Res* **14**, 308–314 (1998).
236. Michelli, M. *Sea-level changes, coastal evolution and paleoceanography of coastal waters in SE Vietnam since the mid-Holocene*. (Christian-Albrechts University, 2008).
237. Abdul, N. A., Mortlock, R. A., Wright, J. D. & Fairbanks, R. G. Younger Dryas sea level and meltwater pulse 1B recorded in Barbados reef crest coral *Acropora palmata*. *Paleoceanography* **31**, 330–344 (2016).
238. Mortlock, R. A., Fairbanks, R. G., Chiu, T. C. & Rubenstone, J. $^{230}\text{Th}/^{234}\text{U}/^{238}\text{U}$ and $^{231}\text{Pa}/^{235}\text{U}$ ages from a single fossil coral fragment by multi-collector magnetic-sector inductively coupled plasma mass spectrometry. *Geochim. Cosmochim. Acta* **69**, 649–657 (2005).
239. Peltier, W. R. & Fairbanks, R. G. Global glacial ice volume and Last Glacial Maximum duration from an extended Barbados sea level record. *Quat. Sci. Rev.* **25**, 3322–3337 (2006).
240. Digerfeldt, G. & Hendry, M. D. An 8000 year Holocene sea-level record from Jamaica: implications for interpretation of Caribbean reef and coastal history. *Coral Reefs* **5**, 165–169 (1987).
241. Toscano, M. A. & Macintyre, I. G. Corrected western Atlantic sea-level curve for the last 11,000 years based on calibrated ^{14}C dates from *Acropora palmata* framework and intertidal mangrove peat. *Coral Reefs* **22**, 257–270 (2003).
242. Gischler, E. Holocene lagoonal development in the isolated carbonate platforms off Belize. *Sediment. Geol.* **159**, 113–132 (2003).
243. Gischler, E. & Hudson, J. H. Holocene development of three isolated carbonate platforms, Belize, Central America. *Mar. Geol.* **144**, 333–347 (1998).
244. Gischler, E. & Hudson, J. H. Holocene development of the Belize Barrier Reef. *Sediment. Geol.* **164**, 223–236 (2004).
245. Gischler, E. & Lomando, A. J. Holocene cemented beach deposits in Belize. *Sediment. Geol.* **110**, 277–297 (1997).
246. Gischler, E. & Lomando, A. J. Isolated carbonate platforms of Belize, Central America: sedimentary facies, late Quaternary history and controlling factors. *Geol. Soc. London, Spec. Publ* **178**, 135–146 (2000).
247. Halley, R. B., Shinn, E. A., Hudson, J. H. & Lidz, B. Recent and relict topography of Boo Bee patch reef, Belize. *Proceedings of the Third International Coral Reef Symposium* **2**, 29–35 (1977).
248. Macintyre, I. G., Littler, M. M. & Littler, D. S. Holocene history of Tobacco Range, Belize, Central America. *Atoll Res. Bull* **430**, 1–18 (1995).
249. Macintyre, I. G., Toscano, M. A., Lighty, R. G. & Bond, G. B. Holocene history of the mangrove and islands of Twin Cays, Belize, Central America. *Atoll Res. Bull* **510**, 18 (2004).
250. Monacci, N. M., Meier-Grünhagen, U., Finney, B. P., Behling, H. & Wooller, M. J. Mangrove ecosystem changes during the Holocene at Spanish Lookout Cay, Belize. *Palaeogeogr. Palaeoclimatol. Palaeoecol.* **280**, 37–46 (2009).
251. Shinn, E. A. *et al.* Geology and sediment accumulation rates at Carrie Bow Cay, Belizein *The Atlantic Barrier Reef Ecosystem at Carrie Bow Cay, Belize, I Structure and Communities* (eds Rützel K., Macintyre I. G.) 63–75 (Smithsonian Institution Press, 1982).
252. Wooller, M. J., Behling, H., Smallwood, B. J. & Fogel, M. Mangrove ecosystem dynamics and elemental cycling at Twin Cays, Belize, during the Holocene. *J. Quat. Sci* **19**, 703–711 (2004).
253. Wooller, M. J., Morgan, R., Fowell, S., Behling, H. & Fogel, M. A multiproxy peat record of Holocene mangrove palaeoecology from Twin Cays, Belize. *The Holocene* **17**, 1129–1139 (2007).
254. Wooller, M. J., Behling, H., Guerrero, J. L., Jantz, N. & Zweigert, M. E. Late Holocene hydrologic and vegetation changes at Turneffe Atoll, Belize, compared with records from mainland Central America and Mexico. *Palaios* **24**, 650–656 (2009).

255. Banks, K. W., Riegl, B. M., Shinn, E. A., Piller, W. E. & Dodge, R. E. Geomorphology of the Southeast Florida continental reef tract (Miami-Dade, Broward, and Palm Beach Counties, USA). *Coral Reefs* **26**, 617–633 (2007).
256. Lighty, R. G., Macintyre, I. G. & Stuckenrath, R. Submerged early Holocene barrier reef south-east Florida shelf. *Nature* **276**, 59–60 (1978).
257. Lighty, R. G., Macintyre, I. G. & Stuckenrath, R. *Acropora palmata* reef framework: a reliable indicator of sea level in the western Atlantic for the past 10,000 years. *Coral Reefs* **125–130** (1982).
258. Multer, H. G., Gischler, E., Lundberg, J., Simmons, K. R. & Shinn, E. A. Key Largo Limestone revisited: Pleistocene shelf-edge facies, Florida Keys, USA. *Facies* **46**, 229–271 (2002).
259. Robbin, D. M. A new Holocene sea-level curve for the upper Florida Keys and Florida reef tract in *Environments of south Florida, present and past* (ed. Gleason P. J.) 437–458 (Miami Geological Society, 1984).
260. Scholl, D. W. & Stuiver, M. Recent submergence of southern Florida: A comparison with adjacent coasts and other eustatic data. *Bull. Geol. Soc. Am* **78**, 437–454 (1967).
261. Stathakopoulos, A. & Riegl, B. M. Accretion history of mid-Holocene coral reefs from the southeast Florida continental reef tract, USA. *Coral Reefs* **34**, 173–187 (2015).
262. Macintyre, I. G., Reid, R. P., Steneck & Robert, S. Growth history of stromatolites in a Holocene fringing reef, Stocking Island, Bahamas. *J. Sediment. Res.* **66**, 231–242 (1996).
263. Adey, W. H. & Burke, R. Holocene bioherms (algal ridges and bank-barrier reefs) of the eastern Caribbean. *Bull. Geol. Soc. Am* **87**, 95–109 (1976).
264. Macintyre, I. G., Raymond, B. & Stuckenrath, R. Recent history of a fringing reef, Bahia Salina del Sur, Vieques Island, Puerto Rico. *Atoll Res. Bull* **268**, 1–9 (1983).
265. Macintyre, I. G. & Glynn, P. W. Evolution of modern Caribbean fringing reef, Galeta Point, Panama. *Am. Assoc. Pet. Geol. Bull* **60**, 1054–1072 (1976).
266. Woodroffe, C. D. Mangrove swamp stratigraphy and Holocene transgression, Grand Cayman Island, West Indies. *Mar. Geol* **41**, 271–294 (1981).
267. Macintyre, I. G. *et al.* Growth and depositional facies of a windward reef complex (Nonsuch Bay, Antigua, WI). in *Proceedings of the Fifth International Coral Reef Congress, Tahiti* 605–610 (1985).
268. Adey, W. H. The algal ridges and coral reefs of St. Croix their structure and Holocene development. *Atoll Res. Bull* **187**, 1–67 (1975).
269. Adey, W. H., Macintyre, I. G., Stuckenrath, R. & Dill, R. F. Relict barrier reef system off St Croix: its implications with respect to Late Cenozoic coral reef development in the western Atlantic. *Proceedings of the Third International Coral Reef Symposium* **2**, 15–21 (1977).
270. Burke, R. B., Adey, W. H. & Macintyre, I. G. Overview of the Holocene history, architecture and structural components of Tague reef and lagoon. *Terr. Mar. Geol. St. Croix, US Virgin Islands. Spec Publ.* **8**, 105–109 (1989).
271. Hubbard, D. K. Holocene reef development along the northeastern St. Croix Shelf, Buck Island, U.S. Virgin Islands. *J. Sediment. Res.* **75**, 97–113 (2005).
272. Macintyre, I. G. & Adey, W. H. Buck Island Bar, St Croix, USVI: a reef that cannot catch up with sea level. *Atoll Res. Bull.* **336**, 330–338 (1990).
273. Macintyre, I. G., Toscano, M. A. & Lundberg, J. Complex environmental patterns and holocene sea level changes controlling reef histories along northeastern St. Croix, USVI. *Atoll Res. Bull.* **556**, 1–27 (2008).
274. Ramcharan, E. K. Mid-to-late Holocene sea level influence on coastal wetland development in Trinidad. *Quat. Int.* **120**, 145–151 (2004).
275. Ramcharan, E. K. & McAndrews, J. H. Holocene development of coastal wetland at Maracas Bay, Trinidad, West Indies. *J. Coast. Res.* **22**, 581–586 (2006).
276. Redfield, A. C. Postglacial change in sea level in the western North Atlantic Ocean. *Science* **157**, 687–692 (1967).
277. Fairbanks, R. G. A 17,000-year glacio-eustatic sea level record: influence of glacial melting rates on the Younger Dryas event and deep-ocean circulation. *Nature* **342**, 637–642 (1989).
278. Weber, J. C. Neotectonics in the Trinidad and Tobago, West Indies segment of the Caribbean-South American plate boundary. *Occas. Pap. Geol. Inst. Hungary* **204**, 21–29 (2010).
279. Kugler, H. G. *Geological map and sections of Trinidad. Scale 1:100,000.* (1961).
280. Toscano, M. A., Macintyre, I. G. & Lundberg, J. Last interglacial reef limestones, northeastern St. Croix, US Virgin Islands—evidence of tectonic tilting and subsidence since MIS 5.5. *Coral Reefs* **31**, 27–38 (2012).
281. Biswas, S. K. Tectonic evolution of the Bengal Foreland Basin since the Early Pliocene and its implication on the development of the Bengal Fan. Recent Geoscientific Studies in the Bay of Bengal and the Andaman Sea, *J. Geol. Soc. India Spl. Pub.* **29**, 5–19 (1992).
282. Montaggioni, L. F. *Recherches géologiques sur les complexes récifaux de l'archipel des Mascareignes (Océan Indien Occidental).* (Marseilles University, 1978).
283. Montaggioni, L. F. Holocene reef growth history in mid-Pacific high volcanic islands. *Proc. 6th Int. Coral Reef Symp. Aust* **3**, 455–460 (1988).
284. Pirazzoli, P. A. & Salvat, B. Ancient shorelines and quaternary vertical movements on Rurutu and Tubuai (Austral isles, French Polynesia). *Zeitschrift für Geomorphol* **36**, 431–451 (1992).
285. Woodroffe, C. D., Short, S. A., Stoddart, D. R., Spencer, T. & Harmon, R. S. Stratigraphy and chronology of late Pleistocene reefs in the Southern Cook Islands, south Pacific. *Quat. Res* **35**, 246–263 (1991).
286. Spencer, T., Stoddart, D. R., Woodroffe, C. D. & Harmon, R. S. Lithospheric flexure and raised reef limestones, S. Cooks-Austral Islands. *Proceeding of the Sixth International Coral Reef Symposium, Australia* **3**, 485–489 (1988).
287. Stoddart, D. R., Spencer, T. & Scoffin, T. P. Reef growth and karst erosion on Mangaia, Cook Islands: A reinterpretation. *Zeitschrift für Geomorphol.* **57**, 1–140 (1985).
288. Spencer, T., Stoddart, D. R. & Woodroffe, C. D. Island uplift and lithospheric flexure: observations and cautions from the South Pacific. *Zeitschrift für Geomorphol.* **63**, 87–102 (1987).
289. Dickinson, W. R. Geomorphology and geodynamics of the Cook Austral island seamount chain in the South Pacific Ocean: implications for hotspots and plumes. *Int. Geol. Rev.* **40**, 1039–1075 (1998).
290. Rashid, R. *et al.* Constraining mid to late Holocene relative sea level change in the southern equatorial Pacific Ocean relative to the Society Islands, French Polynesia, French Polynesia. *Geochimistry, Geophys. Geosystems* **15**, 2601–2615 (2014).
291. Veeh, H. H. $^{230}\text{Th}/^{238}\text{U}$ and $^{234}\text{U}/^{238}\text{U}$ ages of Pleistocene high sea level stand. *J. Geophys. Res.* **71**, 3379–3386 (1966).
292. Schlanger, S. O. *et al.* Site 318: Initial Reports of the Deep-sea Drilling Project, 33. (1976).
293. Talandier, J. & Okal, E. A. Crustal structure in the Society and Tuamotu islands, French Polynesia. *Geophysical J. Int* **88**, 499–528 (1987).
294. Pillans, B. A late Quaternary uplift map for North Island, New Zealand. *R. Soc. New Zeal. Bull* **24**, 409–417 (1986).
295. Browne, G. H. & Naish, T. R. Facies development and sequence architecture of a late Quaternary fluvial-marine transition, Canterbury Plains and shelf, New Zealand: implications for forced regressive deposits. *Sediment. Geol.* **158**, 57–86 (2003).

296. Hijma, M. P. *et al.* A protocol for a geological sea-level database in *Handbook of Sea-Level Research* (eds Shennan I., Long A. J., Horton B. P.) 536–553 (John Wiley and Sons Ltd., 2015).
297. Rovere, A. *et al.* Geo-environmental cartography of the Marine Protected Area 'Isola di Bergeggi' (Liguria, NW Mediterranean Sea). *J. Maps* **6**, 505–519 (2010).
298. Azzopardi, E. & Sayer, M. Estimation of depth and temperature in 47 models of diving decompression computer. *Underw. Technol* **31**, 3–12 (2012).
299. Woodroffe, S. A. *Holocene relative sea-level changes in Cleveland Bay, north Queensland, Australia*. (Durham University, 2006).
300. Morton, R. A. & White, W. A. Characteristics of and corrections for core shortening in unconsolidated sediments. *J. Coast. Res* **13**, 761–769 (1997).
301. Kilbourne, K. H., Quinn, T. M., Guilderson, T. P., Webb, R. S. & Taylor, F. W. Decadal- to interannual-scale source water variations in the Caribbean Sea recorded by Puerto Rican coral radiocarbon. *Clim. Dyn* **29**, 51–62 (2007).
302. Wagner, A. J., Guilderson, T. P., Slowey, N. C. & Cole, J. E. Pre-bomb surface water radiocarbon of the Gulf of Mexico and Caribbean as recorded in hermatypic corals. *Radiocarbon* **51**, 947–954 (2009).
303. Broecker, Wallace, S. & Olson, E. A. Lamont radiocarbon measurements VIII. *Radiocarbon* **3**, 176–204 (1961).
304. Druffel, E. R. M. Radiocarbon in annual coral rings of Belize and Florida. *Radiocarbon* **22**, 363–371 (1980).
305. Druffel, E. R. M. & Linick, T. W. Radiocarbon in annual coral rings of Florida. *Geophys. Res. Lett.* **5**, 913–916 (1978).
306. Druffel, E. R. M. Pulses of rapid ventilation in the North Atlantic surface ocean during the past century. *Science* **275**, 1454–1457 (1997).
307. Southon, J. R., Kashgarian, M., Fontugne, M., Metivier, B. & Yim, W. W.-S. Marine reservoir corrections for the Indian Ocean and southeast Asia. *Radiocarbon* **44**, 167–180 (2002).
308. Wüdsch, M. *et al.* The impact of changing reservoir effects on the ^{14}C chronology of a Holocene sediment record from South Africa. *Quat. Geochronol.* **36**, 148–160 (2016).
309. Dewar, G., Reimer, P. J., Sealy, J. & Woodborne, S. Late-Holocene marine radiocarbon reservoir correction (ΔR) for the west coast of South Africa. *The Holocene* **22**, 1481–1489 (2012).
310. Dutta, K., Bhushan, R. & Somayajulu, B. L. K. ΔR correction values for the northern Indian Ocean. *Radiocarbon* **43**, 483–488 (2001).
311. Hirabayashi, S., Yokoyama, Y., Suzuki, A., Miyairi, Y. & Aze, T. Short-term fluctuations in regional radiocarbon reservoir age recorded in coral skeletons from the Ryukyu Islands in the north-western Pacific. *J. Quat. Sci* **32**, 1–6 (2017).
312. Yoneda, M. *et al.* Radiocarbon marine reservoir ages in the western Pacific estimated by pre-bomb molluscan shells. *Nucl. Instruments Methods Phys. Res. Sect. B Beam Interact. with Mater. Atoms* **259**, 432–437 (2007).
313. Kong, G. S. & Lee, C. W. Marine reservoir corrections (ΔR) for southern coastal waters of Korea. *Sea* **10**, 124–128 (2005).
314. Bolton, A., Goodkin, N. F., Druffel, E. R. M., Griffin, S. & Murty, S. A. Upwelling of Pacific Intermediate Water in the South China Sea revealed by coral radiocarbon record. *Radiocarbon* **58**, 37–53 (2016).
315. Dang, P. X., Mitsuguchi, T., Kitagawa, H., Shibata, Y. & Kobayashi, T. Marine reservoir correction in the south of Vietnam estimated from an annually-banded coral. *Radiocarbon* **46**, 657–660 (2004).
316. Bowman, G. M. Revised radiocarbon oceanic reservoir correction for southern Australia. *Search* **16**, 164–165 (1985).
317. Gillespie, R. & Polach, H. A. The suitability of marine shells for radiocarbon dating of Australian prehistory. in *Proceedings of the 9th International Conference on Radiocarbon Dating* (eds Berger, R. & Suess, H. E.) 404–421 (University of California Press, 1979).
318. Gill, E. D. Australian sea levels in the last 15000 years - Victoria, S.E. Australia. in *Australian sea levels in the last 15,000 years, a review. Monograph Series, Occasional Paper N. 3.* (ed. Hopley, D.) 59–63 (James Cook University, 1983).
319. Bowman, G. M. Oceanic reservoir correction for marine radiocarbon dates from northwestern Australia. *Aust. Archaeol* **20**, 58–67 (1985).
320. O'Connor, S., Ulm, S., Fallon, S. J., Barham, A. & Loch, I. Pre-bomb marine reservoir variability in the Kimberley region, Western Australia. *Radiocarbon* **52**, 1158–1165 (2010).
321. Higham, T. F. G. & Hogg, A. G. Radiocarbon dating of prehistoric shell from New Zealand and calculation of the ΔR value using fish otoliths. *Radiocarbon* **37**, 409–416 (1995).
322. Rafter, T. A., Jansen, H. S., Lockerbie, L. & Trotter, M. M. New Zealand reference standards. in *Proceedings of the 8th International Conference on Radiocarbon Dating H29–H79* (Royal Society of New Zealand, 1972).
323. McSaveney, M. J. *et al.* Late Holocene uplift of beach ridges at Turakirae Head, south Wellington coast, New Zealand. *New Zeal. J. Geol. Geophys* **49**, 337–358 (2006).
324. Sikes, E. L., Samson, C. R., Guilderson, T. P. & Howard, W. R. Old radiocarbon ages in the southwest Pacific Ocean during the last glacial period and deglaciation. *Nature* **405**, 555–559 (2000).
325. Petchey, F., Anderson, A., Zondervan, A., Ulm, S. & Hogg, A. G. New marine ΔR values for the south Pacific subtropical gyre region. *Radiocarbon* **50**, 373–397 (2008).
326. Guilderson, T. P. *et al.* Southwest subtropical Pacific surface water radiocarbon in a high-resolution coral record. *Radiocarbon* **42**, 249–256 (2000).
327. Holden, N. E. Total and spontaneous fission half-lives for uranium, plutonium, americium and curium nuclides. *Pure Appl. Chem.* **61**, 1483–1504 (1989).
328. Meadows, J. W., Armani, R. J., Callis, E. L. & Essling, A. M. Half life of ^{230}Th . *Phys. Rev. C.* **22**, 750–754 (1980).
329. Kopp, R. E., Simons, F. J., Mitrovica, J. X., Maloof, A. C. & Oppenheimer, M. Probabilistic assessment of sea level during the last interglacial stage. *Nature* **462**, 863–867 (2009).
330. Kopp, R. E., Simons, F. J., Mitrovica, J. X., Maloof, A. C. & Oppenheimer, M. A probabilistic assessment of sea level variations within the last interglacial stage. *Geophys. J. Int.* **193**, 711–716 (2013).

Data Citations

1. Hibbert, F. D., Williams, F. H., Fallon, S. J. & Rohling, E. J. *Figshare* <https://doi.org/10.6084/m9.figshare.5367880> (2018).
2. Hibbert, F. D., Williams, F. H., Fallon, S. J. & Rohling, E. J. *Figshare* <https://doi.org/10.6084/m9.figshare.5890567> (2018).
3. Hibbert, F. D., Williams, F. H., Fallon, S. J. & Rohling, E. J. *Figshare* <https://doi.org/10.6084/m9.figshare.5890579> (2018).

Acknowledgements

This work was supported by Australian Laureate Fellowship FL12010050 (E.J.R.). Paula Reimer and Ron Reimer are gratefully acknowledged for constructive discussions regarding aspects of radiocarbon dating. Yusuke Yokoyama (University of Tokyo), Tom Guilderson (University of California, Santa Cruz, Lawrence Livermore National Laboratory), Lucien Montaggioni (Aix-Marseille University), Jody Webster (University of Sydney), Jocelyn Turnbull (Rafter Radiocarbon Laboratory, GNS), Fiona Petchey (Radiocarbon Dating Laboratory, University of Waikato), Adam Switzer (Nanyang Technological

University), Jian-xin Zhao and Nicole Leonard (University of Queensland), Yongqiang Zong (University of Hong Kong), Dennis Hubbard (Oberlin College and Conservatory), Nicole Abdul (Rutgers University), Alessio Rovere (MARUM), Stephan Woodborne (iThemba Laboratories for Accelerator Based Science), Andrew Cooper (Ulster University), Matthew Wooller (University of Alaska, Fairbanks), Tony Belperio (Minotaur Exploration Ltd), Roland Gehrels (University of York), and Kevin Mackay (National Institute of Water and Atmospheric Research, New Zealand) kindly supplied additional information or clarification when requested and are gratefully acknowledged.

Author Contributions

F.D.H. and E.J.R. conceived the scope and design of the study. F.D.H. compiled, entered and edited the data, with specialist contributions from all authors. F.D.H. wrote the data descriptions. F.D.H. led the writing of the manuscript with all authors contributing specialist insights to discussions.

Additional Information

Tables 1, 2, 4, 5, 6 and 7 are only available in the online version of this paper.

Supplementary Information accompanies this paper at <http://www.nature.com/sdata>

Competing interests: The authors declare no competing interests.

How to cite this article: Hibbert F. D. *et al.* A database of biological and geomorphological sea-level markers from the Last Glacial Maximum to present. *Sci. Data* 5:180088 doi: 10.1088/sdata.2018.88 (2018).

Publisher's note: Springer Nature remains neutral with regard to jurisdictional claims in published maps and institutional affiliations.



Open Access This article is licensed under a Creative Commons Attribution 4.0 International License, which permits use, sharing, adaptation, distribution and reproduction in any medium or format, as long as you give appropriate credit to the original author(s) and the source, provide a link to the Creative Commons license, and indicate if changes were made. The images or other third party material in this article are included in the article's Creative Commons license, unless indicated otherwise in a credit line to the material. If material is not included in the article's Creative Commons license and your intended use is not permitted by statutory regulation or exceeds the permitted use, you will need to obtain permission directly from the copyright holder. To view a copy of this license, visit <http://creativecommons.org/licenses/by/4.0/>

The Creative Commons Public Domain Dedication waiver <http://creativecommons.org/publicdomain/zero/1.0/> applies to the metadata files made available in this article.

© The Author(s) 2018